# Lysosomal Acid Lipase Drives Adipocyte Cholesterol Homeostasis and Modulates Lipid Storage in Obesity, Independent of Autophagy

Camille Gamblin, Christine Rouault, Amélie Lacombe, Francina Langa-vives, Dominique Farabos, Antonin Lamaziere, Karine Clément, Emmanuel L Gautier, Laurent Yvan-Charvet, Isabelle Dugail

# Lysosomal acid lipase drives adipocyte cholesterol homeostasis and modulates lipid storage in obesity, independent of autophagy.

Camille Gamblin[1], Christine Rouault[1], Amélie Lacombe[2], Francina Langa-Vives[4], Dominique Farabos[5], Antonin Lamaziere[5], Karine Clément[1], Emmanuel L. Gautier[2], Laurent Yvan-Charvet[3], Isabelle Dugail[1].

[1] UMRS 1269 Inserm/Sorbonne University, Nutriomics, Paris, France
[2] UMRS 1166 Inserm/Sorbonne University, Paris, France
[3] UMRS 1065 Inserm/ Nice Sophia Antipolis University, C3M, Nice, France
[4] Mouse Genetics Engineering Center, Pasteur Institute, Paris, France
[5] Sorbonne University INSERM, Saint Antoine Research center, CRSA, INSERM. Département de Métabolomique Clinique, Hôpital Saint Antoine, AP-HP/Sorbonne Université, Paris, France

Corresponding author: Isabelle.dugail@inserm.fr

Short running title: LAL in adipocyte cholesterol homeostasis

Word count: 3995. References: 33. Figures: 8 Table: 1.

Tweet:
Lysosomal acid lipase drives #adipocyte #cholesterol homeostasis and modulates lipid storage in #obesity, independent of #autophagy. @Nutriomics, @dugaili
Illustration : Fig8G

Abstract

Besides cytoplasmic lipase-dependent adipocyte fat mobilization, the metabolic role of lysosomal acid lipase (LAL), highly expressed in adipocytes is unclear. We show that the isolated adipocyte fraction but not the total undigested adipose tissue from obese patients has decreased LAL expression compared to non-obese. Lentiviral-mediated LAL knockdown in 3T3L1 to mimic obese adipocytes condition did not affect lysosome density or autophagic flux, but increased triglyceride storage and disrupted ER cholesterol as indicated by activated SREBP. Conversely, mice with adipose-specific LAL overexpression (Adpn-rtTA x TetO-hLAL) gained less weight and body fat than controls on a high fat diet, resulting in ameliorated glucose tolerance. Blood cholesterol was lower than controls albeit similar triglyceridemia. Adipose-LAL overexpressing mice phenotype is dependent on the housing temperature, and develops only under mild hypothermic stress (room temperature) but not at thermoneutrality (30°C), demonstrating prominent contribution of BAT thermogenesis. LAL overexpression increased BAT free cholesterol, decreased SREBP targets, and induced the expression of genes involved in initial steps of mitochondrial steroidogenesis, suggesting conversion of lysosome-derived cholesterol to pregnenolone. In conclusion, our study demonstrates that adipose LAL drives tissue cholesterol homeostasis and impacts BAT metabolism, suggesting beneficial LAL activation in anti-obesity approaches aimed at reactivating thermogenic energy expenditure.

## Introduction

Lysosomal acid lipase (Lipa or LAL) is the sole non-polar lipid esterase within lysosomes. Due to human gene mutations, partial inactivation of LAL (as in cholesterol storage disease) or total absence (as in Wolman syndrome) promote ectopic lipid accumulation, hyperlipemia, inflammation and multi-organ (particularly liver) failure (1). According to substrate specificity and pH spectrum, LAL is involved in the utilization of exogenous lipids that enter through receptor-mediated endocytic pathway. As such, LAL regulates macrophage inflammation downstream of lipoproteins endocytosis and efferocytic clearance of apoptotic bodies (2). It is also part of the gene program driving the metabolic switch from a glucose utilizing proinflammatory M1-like macrophage toward a M2-like lipid oxidizing phenotype that promotes tissue remodeling (3). More globally, GWAS analysis of gene variation identified LAL as a susceptibility locus for cardiovascular disease (4), suggesting a role in metabolic regulation.

In the context of diabetes and metabolic diseases, interest in lysosomal lipid hydrolysis has raised following the discovery of lipophagy (5), a LAL-dependent autophagic process for cytoplasmic lipid droplets in which lysosomes ultimately break down triglycerides (TG). Indeed, lipophagy is now recognized a critical step in the control of hepatocyte steatosis, and selective inhibition of liver autophagy produces fatty liver disease in mice (6). It is now recognized that hypothalamic neurons (7) and macrophages (8) also degrade their TG stores by lipophagy, highlighting preference for acid versus neutral lipolysis in some cell types.

Adipocytes, which respond to nutritional inputs by orchestrating lipid mobilization and fatty acid fluxes across the body are essential to maintain metabolic health. Adipose tissue is equipped with highly regulated cytoplasmic lipases that become activated at the lipid droplet surface to fine tune lipid release (9)(10). Despite well-established importance of adipose tissue cytoplasmic lipolysis, high LAL expression is also found in fat cells, which suggests additional roles besides triglyceride mobilization.

Starting from the observation of a decreased adipocyte LAL expression in human obesity, we have investigated the impact of LAL gain and loss of function in cultured fat cells and in mice, which highlights an inverse relationship to adipocyte storage, linked to reorientation of fat cell cholesterol metabolism and thermogenesis, independent of lipophagy. Altogether, our data present an extensive analysis of the impacts of adipocyte LAL modulation, and reveal beneficial metabolic effects of LAL stimulation through cholesterol dynamics.

## Research Design and Methods

*Human adipose tissues*- Subcutaneous adipose tissue from periumbilical region or omentum were excised from obese patients during bariatric surgery at La Pitié-Salpétriere Hospital (Paris), in accordance with local Ethical Committee recommendations (0811792). All participants provided written informed consent. Clinical description (Table1) is provided for two groups according to adipose samples use: direct congelation (group 1, n=45) or collagenase treatment (group 2, n=21). Periumbilical adipose tissue from eight non-obese healthy subjects was obtained by lipoaspiration (Clinique Remusat, Paris, France).

*Sh-mediated LAL downregulation* – 3T3-L1 cells were induced to differentiation with Dexamethasone 1.25µM (Sigma-Aldrich, D1756), IBMX 250µM (Sigma-Aldrich, 15879), Insulin 250nM (Sigma-Aldrich, 19278) for three days followed by insulin alone. 3T3-L1 were transduced with different lentiviral sh vectors (Sigma-Aldrich, 1-TRCN000076829, 2-TRCN000076831, 3-TRCN000076832, 4-TRCN000288217, 5-TRCN000295618) when fully differentiated or as undifferentiated preadipocytes, subsequently selected with puromycin (ThermoFisher, A1113802) to establish stable cell lines

*Autophagic flux* - Cultured cells were serum-starved for 6h before addition or not of lysosome inhibitors: 0.1µM BafilomycinA1 (Sigma-Aldrich, B1793), or 25µM Chloroquine (Sigma-Aldrich, C6628) for 4 hours. P62 and LC3-II were probed by western blotting.

*LAL mouse lines* – TetO-CMV-hLAL mice were obtained by additive transgenesis (Pasteur institute, Paris) by injecting into C57/Bl6J embryos a TRE-CMV promotor upstream of hLAL cDNA, purified from a pTRE2hyg plasmid. Adipose-specific LAL overexpressing mice were generated by breeding Adpn-rtTa mice with TetO-CMV-hLAL and genotyping with 5'-AGCCCAGTGTAAAGTGGCCC-3' 5'-CTGGACAAGAGCAAAGTCAT-3' and 5'-TGTGCCTTAACCGAATTCCT-3' 5'-CTGGTTTGGGACCTTTGTCA-3'. Weaned littermates were fed HFD (Research Diet, D12492i) with free access to drinking water containing 1g/L Doxycycline (Sigma-Aldrich, D9891).

*Mice phenotyping* – Mice were housed at room temperature (22°C) or thermoneutrality (30°C) in a climate chamber (TSE, PhenoMaster). Body composition was analyzed by nuclear magnetic resonance (Bruker Mouse Minispec, LF90). Blood and fat pads (gonadal (OvAT-EpiAT), subcutaneous (ScAT), brown adipose tissue (BAT)) were frozen in liquid nitrogen or fixed with Formalin (Sigma Aldrich, HT501128), or incubated with collagenase as described (11). Oral glucose tolerance test (OGTT) started by gavage with 2.0 g/kg glucose in mice fasted for 6h. Glycemia was followed with a sugar test meter (ACCU-CHECK, Roche). Serum steroid profiling was measured by LC/MS-MS according to established methods (12)

*Indirect calorimetry* – Mice were acclimated in individual cages for 2 days before measurement of $VO_2$, $VCO_2$, locomotor activity, food and water consumption over 5 consecutive days at 22°C (PhenoMaster, TSE). HFD and Doxycycline were maintained.

*Gene and Protein expression* - Total RNA was extracted using an RNeasy Mini kit (Qiagen, 74104), followed by Quantitative real-time PCR using Master Mix (Applied Biosystems). Lysates in RIPA buffer (Sigma Aldrich, R0278) containing proteinase inhibitors (Complete Mini, Roche) were prepared (Bertin Technologies, Precellys 24) and cleared for 10min at 10.000rpm. Protein concentration was measured (ThermoFisher Scientific, BCA assay). western blotting was performed as described (13).

*Adipose tissue lipolysis – Cultured adipocytes or* ScAT fragments were incubated into DMEM containing 1% bovine Serum Albumin (Sigma-Aldrich, A8806) for 2h at 37°C with or without 10µM Isoproterenol (Sigma-Aldrich, 1351005). Released glycerol was measured with Free Glycerol reagent (Sigma-Aldrich, F6428). Frozen tissues were used to determine cholesterol (Amplex red kit, Invitrogen, A12216) or triglyceride (Cayman, 10010303) contents.

*Statistical Analysis - U*npaired two-tailed t tests, ANOVA analysis, Mann Whitney non-parametric tests or Spearman correlations were performed with GraphPad Prism 7.

*Data and resources availability* - TetO-CMV-hLAL mouse strain generated during the current study is available from the corresponding author upon request.

**Results**

*Decreased adipocyte -but not whole adipose tissue- LAL expression in human obesity.*

Adipose tissue LAL expression is poorly documented. In mice, positive association to body weight was reported, with elevated *Lipa* mRNA in obese compared to lean fat pads (14). In agreement, we have observed increased Lipa mRNA in the fat tissue of mice made obese by high fat diet feeding compared to lean animals fed chow *(Figure 1A)*. Moreover, microarray analysis of human subcutaneous adipose tissue LIPA expression replicated on 2 independent groups of obese (BMI>30Kg/m2) compared to non-obese subjects (BMI<30Kg/m2) indicated significantly upregulated LIPA signal in obese patients (fold change 1.55 and 1.07; q value 0.031 and 0.005 respectively). To pinpoint the origin of this regulation, we first analyzed *Lipa*

expression in the main cell sub-populations comprised in mice adipose tissue i.e. mature adipocytes or the different cell types in SVF separated by FACs as previously described (15). We observed comparable *Lipa* expression in floating adipocytes, endothelial cells ($Cd45^-$ $Cd31^+$) and resident macrophages ($Cd45^+$ $F4/80^+$), but very low mRNA levels in progenitor cells defined as $Cd45^-Cd31^-Cd140^+$ *(Figure 1B)*. This suggested that cell composition, especially the adipose versus non-adipose cell ratio might be a strong determinant of tissue LAL expression. In non-obese subjects or patients with massive obesity (mean BMI 47 $Kg/m^2$, Table 1) SVF LIPA mRNA was independent of the BMI of the donor on a per cell basis *(Figure 1C)*. This suggested that up-regulation of LAL expression with obesity is linked to the number of stromal cells present in fat, especially infiltrated macrophages. Importantly, contrary to stromal LAL, obesity modulated floating adipocyte expression, and LIPA mRNA was lower in obese compared to lean adipocytes *(Figure 1D)*. Within the bariatric obese cohort in which two distinct fat tissue depots (subcutaneous and omental) could be sampled in the same patient, adipocyte LIPA mRNA was highly concordant between fat locations *(Figure 1E)*. Unfractionated adipose tissue biopsies, available in a separate group of obese patients with very similar characteristics *(Table 1)* did not revealed links between LIPA expression and indicators of obesity severity (body weight, BMI or total fat mass), but showed positive correlation with markers of obesity-related dysfunction such as android fat distribution or circulating ASAT *(Figure 1F)*. These findings indicate that total adipose tissue LAL is a marker of metabolic impairment in obesity, rather than an indicator of obesity severity.
Thus, these experiments reveal a complex pattern of obesity-related adipose LAL regulation, with a strong dependence on tissue composition with regard to non-adipose cells, concomitant with a deficit of LAL expression in mature adipocytes. They highlight the need for cell type-specific studies to address the question of the significance of adipocyte LAL.

*Adipocyte LAL down-regulation by lentiviral shRNA promotes fat accumulation and affects lipid droplet dynamics, independent of autophagy.*

To explore the consequences of obesity-linked adipocyte LAL down-regulation, we modulated LAL expression using lentiviral vectors to reduce LAL in fully differentiated lipid-laden 3T3-L1 cells, a recognized model for fat cells. Five days after differentiation, when clearly visible lipid droplets had accumulated, cells were transduced with five different sh lentiviral stocks or no virus, and LAL expression was assessed after additional 7days. Among five sequences, two (sh3 and sh4) inhibited LAL expression with more than 50% efficiency, whereas the other three (sh1-2-5) showed slight or no inhibition *(Figure 2A)*. Cells treated with sh3-4 were analyzed together and thereafter denominated Lipa sh, whereas cells treated with inactive sh1-2-5 were considered sh controls. Similar to that reported in genetically or pharmacologically LAL-deficient macrophages (16) adipocyte LAL down-regulation raised total cholesterol cell contents *(Figure 2B)*. Further, high doses of oxidized LDL (Ox-LDL), known to inhibit LAL activity (17) increased cholesterol contents in LAL expressing adipocytes up to the level of Lipa Sh cells *(Figure 2B)*. Thus, as a hallmark of LAL functional impairment cholesterol loading is seen in both OxLDL treatment and lentivirus-mediated *Lipa* knockdown.
Not only cholesterol esters but also TG are LAL substrates. Despite unaffected expression of cytoplasmic lipases and lipid droplet-coating *Plin1 (Supplemental Figure 1A)*, or adipocyte specific genes *(Supplemental Figure 1B)*, we found that TG contents were higher in Lipa sh cells compared to control sh or untransfected cells *(Figure 2C)*. Perilipin1 protein content increased in Lipa sh compared to controls *(Figure 2D)*, further indicating lipid droplet accumulation. Thus, LAL down-regulation favors adipocyte TG storage.

We next generated stable shRNA *Lipa* knock-down by puromycin selection, in which low levels of LAL mRNA were maintained before (D0) or after (D7) full differentiation *(Supplemental Figure 1C)*. Overall fat cell conversion was unaffected, as indicated by normal adipocyte markers expression *(Supplemental Figure 1D)*. Lysosome integrity and density was conserved as shown by protein contents of lysosome chaperones Lamp2A and Hsc70 *(Supplemental figure 1E)* and pulse-chase labeling with Dextran-Texas Red *(Figure 2E)*. Autophagosome marker (LC3-II) or autophagic substrate (p62) contents were also similar in control and LAL-deficient cells *(Supplemental figure 1F)*. Treatment with lysosome inhibitors (Chloroquine (CQ) and BafilomycinA1 (BAF)) to assess autophagic flux showed equivalent accumulation rates of p62 and LC3-II *(Figure 2F-H)*, indicating unaffected lysosomal clearance in LAL-deficient conditions. Regarding lipolysis, the presence of BAF did not affected basal glycerol release, which was also not different in LAL deficient and in controls (*Figure 2I-J*). BAF only slightly inhibited isoproterenol-stimulated lipolysis by less than 25% in control adipocytes (*Figure 2K* and previous data (12)), an effect that was also observed in LAL deficient cells (*Figure 2K*), suggesting a lipophagy-unrelated action. Of note, lysosome inhibitors did not affect Perilipin1 contents (not shown), indicating that the adipocyte-specific isoform is not degraded in lysosomes, contrary to that shown for non-adipose perilipin-2 and -3 (18). Thus, the impact of LAL downregulation in adipocytes is autophagy-independent.

We next investigated potential changes in cell cholesterol homeostasis, revealed by Sterol Regulatory Element Binding Protein status. As a cholesterol-regulated transcription factor, auto-regulated SREBP2 and its target genes (HMG-CoA reductase, LDL receptor) are induced in response to cholesterol depletion sensed in the endoplasmic reticulum (ER). Independently generated stable transfectants were stratified into 3 groups based on residual levels of *Lipa* expression *(Figure 3A)*, in which *Hmgcr*, *Srebf2* and *Ldlr* mRNA levels gradually increased with stronger LAL knockdown, suggesting a state of ER-sensed cholesterol depletion in LAL deficiency *(Figure 3B)*. Indeed, residual *Lipa* expression negatively correlated with *Srebf2* gene expression, the lower *Lipa* mRNA, the higher *Srebf2 (Figure 3C)*, and also varied inversely to *Fasn,* a SREBP-regulated lipogenic gene (S*upplemental figure 2A*). Cell replenishment with a bolus of a free cholesterol supplemented medium, followed by a 4-hour chase in standard medium was sufficient to abolish differences in *Srebf2* and *Hmgcr* mRNA between *Lipa* groups (*Figure 3D, Supplemental figure 2B)*, suggesting that restrained LAL-dependent free cholesterol delivery to the ER was most likely the cause of upregulated expression of cholesterol-regulated genes.

As cholesterol-sensitive ER is also the site of lipid droplet (LD) assembly and budding, we probed for altered topology of TG accumulation by LAL deficiency. Concomitant with elevated TG contents and LD-associated perilipin fluorescence in Sh Lipa compared to Sh controls *(Figure 3E)*, we also found increased FAS protein contents in Lipa deficient cells, indicative of active lipogenesis (*Figure 3F*). Unexpectedly the mean diameter of LDs proportionally declined with *Lipa* inhibition. ANOVA analysis of more than 10.000 single LDs from independent cell pools indicated significant negative contribution of LAL deficiency to LD size *(Figure 3G)*. This infers that the number of LD per cell increases in LAL deficient adipocytes, as more lipid were accommodated in smaller LDs. However, because LDs are so numerous and heterogeneous in differentiated 3T3-L1 adipocytes, direct measure of the total number of LDs per cell requires 3D reconstitution of images, difficult to accurately analyze in a sufficient number of cells. Although not directly evaluated, we suggest that an increased in the number of LDs could be linked to facilitated LD budding from cholesterol-depleted ER. Other ER functions, such as the UPR (Unfolded Protein Response) remained unaffected by LAL deficiency, as a normal response to an UPR inducer (Dithiothreitol) which disrupts oxidative protein folding in the ER

lumen, was mounted irrespective of *Lipa* expression *(Figure 3H-I)*. Together, these data underline LAL-dependence of a specific cholesterol lysosome to ER axis in regulating adipocyte homeostasis. We propose that defective cholesterol esters hydrolysis in LAL deficit could limit free cholesterol exit from lysosomes, and induce a chronic state of cholesterol demand in the ER, in favor of LD budding.

*Adipocyte LAL overexpression in mice alleviates high fat diet induced obesity and metabolic complications.*

We next generated mice with adipocyte-specific LAL overexpression to investigate the impact of adipocyte LAL modulation at whole-body level. We bred Adpn-rtTA mice with TetO-CMV-hLAL, and fed littermates on a high fat diet (HFD) for 12 weeks with free access to doxycycline-supplemented drinking water (1g/l). We used primers recognizing both the hLAL transgene and the endogenous mouse *Lipa* mRNA to confirm significant over-expression of LAL in adipose tissues *(Figure 4A)*. Compared to control single transgenics (*Adpn*$^{+}$*/LAL*$^{-}$ or *Adpn*$^{-}$*/LAL*$^{+}$) a significant increase in LAL expression was seen in *Adpn*$^{+}$*/LAL*$^{+}$ female adipose tissues but not in the liver, as expected. In males, due to high levels of endogenous LAL in the epididymal fat (EpiAT), overexpression was seen only in brown (BAT) and subcutaneous (ScAT) depots *(Figure 4B)*. *Adpn*$^{+}$*/LAL*$^{+}$ livers of male mice expressed unpredicted high LAL mRNA compared to controls. Thus, considering sex-specific responses, we decided to limit analysis to female only, in which transgene-driven adipocyte LAL expression was robust and consistent *(Figure 4C)*.

LAL overexpressing *Adpn*$^{+}$*/LAL*$^{+}$ female mice gained less weight than *Adpn*$^{-}$*/LAL*$^{+}$ or *Adpn*$^{+}$*/LAL*$^{-}$ controls on a 12-weeks HFD *(Figure 4D)*. Analysis of body composition indicated decreased fat mass, but not lean mass or fluids *(Figure 4E)*, and less developed OvAT and ScAT depots *(Figure 4F)*. Because LAL has TG lipase activity, we checked for stimulation of adipocyte TG mobilization to explain lower fat deposition. Basal glycerol release by *ex vivo* ScAT fragments was similar regardless the donor mice genotype or diet (chow diet or HFD). Maximally stimulated lipolysis with isoproterenol was also unaffected *(Figure 4G)*. Thus, the lean phenotype of LAL overexpressing mice is unrelated to adipocyte lipolysis and TG mobilization.

In line with their lower fat mass, LAL overexpressing mice were also less prone to HFD-dependent visceral adipose tissue inflammation and expressed less *Cd68*, *Il6* and *Tnfa* mRNA than controls *(Figure 5A)*. We also found elevated *Scd1* (StearoylCoa desaturase1) mRNA expression in the OvAT of *Adpn*$^{+}$*/LAL*$^{+}$ mice *(Supplemental figure 3A)*, which translated into a greater proportion of monounsaturated fatty acids at the expense of saturated fatty acids *(Supplemental Figure 3B-C)*. High ratio of monounsaturated over saturated fatty acids is metabolically beneficial, as well as low adipose tissue inflammation, which prompted us to check glucose homeostasis in LAL overexpressing mice. Compared to controls, *Adpn*$^{+}$*/LAL*$^{+}$ mice had lower fasting blood glucose *(Figure 5B)*, and their glycemic response to an oral glucose load (OGTT) was less *(Figure 5C)*. Noticeably, a highly significant correlation between glycemia and circulating cholesterol concentrations was found *(Figure 5D)*, and *Adpn*$^{+}$*/LAL*$^{+}$ mice had lower blood cholesterol than controls *(Figure 5E)* despite comparable triglyceridemia *(Figure 5F)*. All together, these data indicate a beneficial impact of adipocyte LAL overexpression to damper the deleterious metabolic consequences of HFD.

*Improvement of metabolic response in adipocyte LAL overexpression is linked to thermogenesis.*

To investigate the cause of LAL-mediated obesity resistance upon HFD feeding in mice, we assessed energy balance components by indirect calorimetry. We explored *Adpn*$^{+}$*/LAL*$^{+}$ mice against *Adpn*$^{-}$*/LAL*$^{+}$ controls, and found similar food intake and locomotor activity in the two groups *(Figure 5G)* but energy expenditure profiles in *Adpn*$^{+}$*/LAL*$^{+}$ were above controls *(Figure 5H)*. This suggested a role for thermogenesis, a prominent energy expense module required to defend mice core temperature in standard housing conditions (22°C). LAL expression in BAT inversely correlated with body weight response to HFD *(Figure 5I)*, which further suggests BAT contribution. To decipher the role of BAT-related thermogenesis in the obesity-resistant phenotype of LAL overexpressing mice, we reevaluated mice fed a HFD as above, but housed under thermoneutral conditions (i.e. 30°C instead of 22°C) to shut-off thermogenic response. LAL overexpression persisted in thermoneutrally housed *Adpn*$^{+}$*/LAL*$^{+}$ *mice (Figure 6A)* and BAT morphology showed expected differential lipid accumulation after 4 weeks of conventional versus thermoneutral housing *(Figure 6B)*. Within this 4-week period, we did not observed differences in cumulative weight gains between thermoneutral and conventional control groups, but body weights poorly segregated among genotypes in thermoneutral mice, whereas differences had clearly established in mice raised conventionally *(Figure 6C)*. Furthermore, even if a small difference in body weight still persisted between thermoneutral *Adpn*$^{+}$*/LAL*$^{-}$ and *Adpn*$^{+}$*/LAL*$^{+}$ groups, this was not related to lower fat mass, but decreased in lean mass preexisting before thermoneutrality was applied *(Figure 6D)*. Lowering of cholesterolemia in conventionally raised LAL overexpressing mice *(Figure 5E)* was no longer present after thermoneutral housing (*Figure 6E)*, nor amelioration of glucose tolerance *(Figure 6F)*. Thus, LAL mice phenotype is highly dependent on housing temperature, which demonstrated a role for adipocyte thermogenic activity and led us to focus on brown/beige adipose tissue depots as preferential functional targets of LAL overexpression.

*LAL overexpression modulates adipocyte cholesterol homeostasis and induces mitochondrial steroidogenesis.*

Investigating BAT closer, we found no significant change in TG contents between *Adpn*$^{+}$*/LAL*$^{+}$ and control mice *(Figure 7A)*, but free cholesterol was increased in the BAT of LAL overexpressing mice *(Figure 7B)*. Free cholesterol represents the major fraction of total cholesterol in BAT (81.7+/-6.1% and 83.0+/-3.7% in *Adpn*$^{+}$*/LAL*$^{+}$ and controls respectively), far above the esterified cholesterol form *(Figure 7B insert)*. Selective impact on BAT was suggested, as no change with LAL overexpression was found in the white OvAT *(Supplemental figure 4)*. In BAT of *Adpn*$^{+}$*/LAL*$^{+}$ mice, cholesterol-regulated *Ldlr* and *Hmgcr* mRNA expression genes were down-regulated compared to controls, and *Srebf2* expression followed the same trend, although not reaching the statistical significance threshold *(Figure 7C)*. Genes controlling cholesterol efflux (*Abca1* and *Scarb1*) were not induced *(Figure 7D),* consistent with tissue free cholesterol accumulation. We also observed that compared to control BAT, LAL overexpressing BAT expressed lower levels of ER stress markers, suggesting ameliorated metabolic adaptation *(Figure 7E)*. In agreement, BAT *Ucp1*mRNA expression positively associated with LAL expression *(Figure 7F)*. Regarding ScAT, a white fat depot in which brown-like adipocytes can develop (a process called fat beiging) we could also detect positive *Ucp1* mRNA expression in 40% of the *Adpn*$^{+}$*/LAL*$^{+}$ mice, compared to less than 10% in controls *(Figure 7G)*. Also, a trend toward higher proportion of fat tissue positive for *Cidea* and *Dio2* mRNA was found in SCAT of *Adpn*$^{+}$*/LAL*$^{+}$ (*Figure 7G*), suggesting a higher potential for beiging. Together these data indicate that LAL overexpression improved thermogenic potential.

BAT activation fits with a leaner phenotype of LAL overexpressing mice on HFD, but surprisingly coexists with tissue free cholesterol accumulation, which is usually considered a deleterious condition for mitochondrial function (19). Nonetheless, the inner mitochondrial membrane is equipped with a steroidogenic enzyme machinery, which transforms free cholesterol into steroids, a pathway that has the potential to alleviate mitochondrial cholesterol overload. The gene encoding the first step in steroidogenesis, the mitochondrial P450 side-chain cleavage enzyme *Cyp11a1*, which converts cholesterol into pregnenolone is expressed in brown adipocytes (20). We found that the expression of this steroidogenic genes: *Cyp11a1* as well as its upstream transcriptional regulator *Nr5a1 (*known as steroidogenic factor 1) were upregulated in BAT of LAL overexpressing mice *(Figure 7H)*. In addition, BAT *Nr5a1* expression positively associated with LAL *(Figure 7I)*, and was negatively linked to body weight gain on HFD *(Figure 7J)*. Mass spectrometry profiling of serum steroids indicated a trend towards higher pregnenolone and 17-OH pregnenolone concentrations in LAL overexpessing mice compared to controls *(Figure 8A-B)*. Further, 5α-dihydrotestosterone (5ADT) and testosterone, downstream products of pregnenolone in the sex hormone branch of steroidogenesis were significantly higher in *Adpn*$^{+}$*/LAL*$^{+}$ mice serum *(Figure 8C-D). 17OH-pregnenolone* and 5ADT positively correlated with BAT *Nr5a1* mRNA expression *(Figure 8E-F)*. Other serum metabolites in the corticosteroid or mineralosteroid pathways remained unchanged in the two groups of mice (not shown). Altogether, these data reveal induction of BAT mitochondrial steroidogenesis, likely an adaptive response to accelerated cholesterol utilization in BAT following LAL overexpression. This potentially explains why mitochondrial function is preserved in cholesterol laden BAT of LAL overexpressing mice. It also provides a molecular basis for the role of BAT as a cholesterol sink, which remain to be further characterized.

**Discussion**

Our study brings novel insights into the unappreciated role of adipocyte lysosomal lipase in energy balance regulation. Previous report in mice with LAL global loss of function demonstrated lipotoxic fattening of organs, especially liver and intestine (21). As models for life threatening Wolman disease in patients, these mice could be normalized by hepatocyte LAL rescue (22). Also, liver-specific gene deletion of LAL revealed that cholesterol esters were the most prominent lipids accumulated in hepatocytes, far above triglycerides and retinyl esters, other *in vitro* LAL substrates (23). Global LAL deficiency was reported to cause disappearance of adipose tissue stores (21), which led to the conclusion that LAL positively regulated adipose tissue storage. However, lipoatrophy in global LAL deficiency is paradoxical, largely due to malabsorptive cachexia and liver failure at the end point of disease development. More recently, it was shown that fat mass was still preserved in young LAL-deficient mice, but reported hypothermic events and defective brown adipose tissue thermogenesis (24), which is in line with our present observations.

Our data reveal a metabolic role of adipose LAL modulation. We demonstrate that LAL regulates energy expenditure and subsequent adipose tissue triglyceride storage, primarily as a gatekeeper of lysosome cholesterol exit for delivery into adipocytes. When adipocyte LAL expression decreases, cholesterol delivery from lysosomes to ER is reduced, which in turn activates cholesterol-dependent SREBP and subsequent fat storage. On the contrary, LAL overexpression, by increasing the turnover of cholesterol through the lysosomal-ER axis, promotes beneficial brown fat activity and a mitochondrial steroidogenic pathway. LAL knock-down in adipose cell lines and overexpression in mice led to apparently different end points (increased fat storage or activated BAT thermogenesis) which can appear unrelated one from

the other. However a common pattern in these two opposite situations is the modulation of cholesterol-dependent SREBP pathway *(Figure 8G).* A limitation of our study is lack of information on LAL protein levels or enzyme activity. We could not validate consistent LAL immunoreactivity in adipose tissue extracts despite attempts with several commercial antibodies. Accurate measurement of enzyme activity was also confounded by the unusual status of adipose tissue lipase equipment, which contains, in addition to LAL, a large variety of other very abundant lipases that can still exhibit residual activity at acidic pH. In such a context of tissue equipment with diverse lipases, the accuracy of Lalistat, the "specific" LAL inhibitor is not validated, and the artificial LAL substrate designed in the LAL assay is competed by uncontrolled adipose TG, which further confounds enzyme activity determination.

Our data highlight LAL-dependent regulation of adipocyte cholesterol balance, in line with previous studies on the importance of ABCA1 (25) and ABCG1-mediated cholesterol efflux (26) in fat cell lipid storage. LAL-dependent cholesterol regulation is closely linked to a unique adipocyte low capacity for endogenous cholesterol synthesis (27)(28), leading to inability to restore homeostasis with *de novo* synthetized cholesterol. The LAL-dependent pathway for exogenous cholesterol delivery to adipocytes is responsive to nutritional overload in obesity. We show here that in mice on HFD, BAT cholesterol content is LAL-dependent, as well as body weight gain. Although direct subcellular localization of cholesterol accumulation upon LAL manipulations would have reinforced our conclusions, indirect biochemical quantifications confirm that free cholesterol is indeed accumulated in LAL overexpressing fat cells. Together with BAT cholesterol accumulation in LAL overexpressing mice, we found lower cholesterolemia which might suggest that activated BAT serves as a metabolic sink for cholesterol, as it does for glucose, fatty acids (29) and branched chain amino acids (30). Indeed, protective brown fat activation against hypercholesterolemia has been proposed (31). LAL is required for lipophagy, but we found autophagy-independent LAL-dependent regulation in adipocytes. This fits with a minor role of adipocyte autophagic degradation of lipid droplets in face of the prominent importance of cytoplasmic lipases for adipocyte TG mobilization, even if autophagic clearance of other cell components is central for adipocyte maintenance and response to obesity (32) (33)(13).

By exploring LAL status of human adipocytes, we show that as far as the confounding contribution of adipose tissue macrophage LAL is eliminated, LAL expression is reduced in obese adipocytes, which opens the perspective of therapeutic LAL activation. With brown fat as a preferred adipose target, LAL activation could ameliorate metabolic condition in obese subjects if combined with interventions aimed at favoring brown/beige fat stimulation. Further, beneficial lowering of blood cholesterol levels could be expected from the mouse study. Association between cholesterolemia and adipocyte LAL in the obese population explored here could not be investigated because most patients were under statin treatment. Altogether, our present observations argue for considering LAL activation in the obese setting as a strategy to implement protective effects of brown fat activation against metabolic disorders.

**Acknowledgments**. Adpn-rtTa mice were provided by P. Scherer. We thank the members of the Mouse Genetics Engineering of the Institut Pasteur for technical support with transgenic mice. Marie Lhomme (ICAN Analytics Lipidomic facility,La Pitié-Salpetrière, Paris) is acknowledged for providing fatty acid analysis.

Author contribution: CG, CR, AL, FLV performed the experiments. KC, ELM, LYC an ID designed the experiments and wrote the manuscript. ID is the guarantor of the study.

The funding of National Research Agency (ANR-14-CE12-0017, LIPOCAMD) is

acknowledged. No conflict of interest is declared.

**Reference List**

1. Burton BK, Deegan PB, Enns GM, Guardamagna O, Horslen S, Hovingh GK, et al. Clinical Features of Lysosomal Acid Lipase Deficiency. J Pediatr Gastroenterol Nutr. 2015;61(6):619–25.
2. Viaud M, Ivanov S, Vujic N, Duta-Mare M, Aira L-E, Barouillet T, et al. Lysosomal Cholesterol Hydrolysis Couples Efferocytosis to Anti-Inflammatory Oxysterol Production. Circ Res. 2018;122(10):1369–84.
3. Huang SCC, Everts B, Ivanova Y, O'Sullivan D, Nascimento M, Smith AM, et al. Cell-intrinsic lysosomal lipolysis is essential for alternative activation of macrophages. Nat Immunol. 2014;15(9):846–55.
4. Coronary Artery Disease (C4D) Genetics Consortium. A genome-wide association study in Europeans and South Asians identifies five new loci for coronary artery disease. Nat Genet. 2011;43(4):339–44.
5. Zechner R, Madeo F. Cell biology: Another way to get rid of fat. Vol. 458, Nature. 2009. p. 1118–9.
6. Singh R, Kaushik S, Wang Y, Xiang Y, Novak I, Komatsu M, et al. Autophagy regulates lipid metabolism. Nature. 2009;458(7242):1131–5.
7. Coupé B, Ishii Y, Dietrich MO, Komatsu M, Horvath TL, Bouret SG. Loss of autophagy in pro-opiomelanocortin neurons perturbs axon growth and causes metabolic dysregulation. Cell Metab. 2012;15(2):247–55.
8. Ouimet M, Franklin V, Mak E, Liao X, Tabas I, Marcel YL. Autophagy regulates cholesterol efflux from macrophage foam cells via lysosomal acid lipase. Cell Metab. 2011;13(6):655–67.
9. Schweiger M, Schreiber R, Haemmerle G, Lass A, Fledelius C, Jacobsen P, et al. Adipose triglyceride lipase and hormone-sensitive lipase are the major enzymes in adipose tissue triacylglycerol catabolism. J Biol Chem. 2006;281(52):40236–41.
10. Zimmermann R, Strauss JG, Haemmerle G, Schoiswohl G, Birner-Gruenberger R, Riederer M, et al. Fat mobilization in adipose tissue is promoted by adipose triglyceride lipase. Science (80- ). 2004;306(5700):1383–6.
11. Marcelin G, Da Cunha C, Gamblin C, Suffee N, Rouault C, Leclerc A, et al. Autophagy inhibition blunts PDGFRA adipose progenitors' cell-autonomous fibrogenic response to high-fat diet. Autophagy. 2020;
12. Fiet J, Bouc Y Le, Guéchot J, Hélin N, Maubert MA, Farabos D, et al. A liquid chromatography/tandem mass spectometry profile of 16 serum steroids, Including 21-Deoxycortisol and 21-deoxycorticosterone, for management of congenital adrenal hyperplasia. J Endocr Soc. 2017;1(3):186–201.
13. Soussi H, Reggio S, Alili R, Prado C, Mutel S, Pini M, et al. DAPK2 downregulation associates with attenuated adipocyte autophagic clearance in human obesity. Diabetes. 2015;64(10):3452–63.
14. Xu X, Grijalva A, Skowronski A, Van Eijk M, Serlie MJ, Ferrante AW. Obesity activates a program of lysosomal-dependent lipid metabolism in adipose tissue macrophages independently of classic activation. Cell Metab. 2013;18(6):816–30.
15. Marcelin G, Ferreira A, Liu Y, Atlan M, Aron-Wisnewsky J, Pelloux V, et al. A PDGFRα-Mediated Switch toward CD9highAdipocyte Progenitors Controls Obesity-Induced Adipose Tissue Fibrosis. Cell Metab. 2017;25(3):673–85.
16. Schlager S, Vujic N, Korbelius M, Duta-Mare M, Dorow J, Leopold C, et al. Lysosomal lipid hydrolysis provides substrates for lipid mediator synthesis in murine macrophages. Oncotarget. 2017;8(25):40037–51.
17. Heltianu C, Robciuc A, Botez G, Musina C, Stancu C, Sima A V., et al. Modified Low Density Lipoproteins Decrease the Activity and Expression of Lysosomal Acid Lipase in Human Endothelial and Smooth Muscle Cells. Cell Biochem Biophys. 2011;61(1):209–16.
18. Kaushik S, Cuervo AM. Degradation of lipid droplet-associated proteins by chaperone-

mediated autophagy facilitates lipolysis. Nat Cell Biol. 2015;17(6):759–70.
19. Echegoyen S, Oliva EB, Sepulveda J, Diaz-Zagoya JC, Espinosa-Garcia MT, Pardo JP, et al. Cholesterol increase in mitochondria: Its effect on inner-membrane functions, submitochondrial localization and ultrastructural morphology. Biochem J. 1993;289(3):703–8.
20. Li J, Daly E, Campioli E, Wabitsch M, Papadopoulos V. De novo synthesis of steroids and oxysterols in adipocytes. J Biol Chem. 2014;289(2):747–64.
21. Du H, Heur M, Duanmu M, Grabowski GA, Hui DY, Witte DP, et al. Lysosomal acid lipase-deficient mice: depletion of white and brown fat, severe hepatosplenomegaly, and shortened life span. J Lipid Res. 2001;42(4):489–500.
22. Du H, Zhao T, Ding X, Yan C. Hepatocyte-Specific Expression of Human Lysosome Acid Lipase Corrects Liver Inflammation and Tumor Metastasis in lal-/-Mice. Am J Pathol. 2015;185(9):2379–89.
23. Pajed L, Wagner C, Taschler U, Schreiber R, Kolleritsch S, Fawzy N, et al. Hepatocyte-specific deletion of lysosomal acid lipase leads to cholesteryl ester but not triglyceride or retinyl ester accumulation. J Biol Chem. 2019;294(23):9118–33.
24. Duta-Mare M, Sachdev V, Leopold C, Kolb D, Vujic N, Korbelius M, et al. Lysosomal acid lipase regulates fatty acid channeling in brown adipose tissue to maintain thermogenesis. Biochim Biophys Acta - Mol Cell Biol Lipids. 2018;1863(4):467–78.
25. Le Lay S, Robichon C, Le Liepvre X, Dagher G, Ferre P, Dugail I. Regulation of ABCA1 expression and cholesterol efflux during adipose differentiation of 3T3-L1 cells. J Lipid Res. 2003;44(8).
26. Frisdal E, Le Lay S, Hooton H, Poupel L, Olivier M, Alili R, et al. Adipocyte ATP-binding cassette G1 promotes triglyceride storage, fat mass growth, and human obesity. Diabetes. 2015;64(3).
27. Le Lay S, Ferré P, Dugail I. Adipocyte cholesterol balance in obesity. Biochem Soc Trans. 2004;32(1):103–6.
28. Dugail I, Le Lay S, Varret M, Le Liepvre X, Dagher G, Ferré P. New insights into how adipocytes sense their triglyceride stores. Is cholesterol a signal? Horm Metab Res. 2003;35(4):204–10.
29. Cypess AM, Lehman S, Williams G, Tal I, Rodman D, Goldfine AB, et al. Identification and importance of brown adipose tissue in adult humans. N Engl J Med. 2009;360(15):1509–17.
30. Yoneshiro T, Wang Q, Tajima K, Matsushita M, Maki H, Igarashi K, et al. BCAA catabolism in brown fat controls energy homeostasis through SLC25A44. Nature. 2019;572(7771):614–9.
31. Berbeé JFP, Boon MR, Khedoe PPSJ, Bartelt A, Schlein C, Worthmann A, et al. Brown fat activation reduces hypercholesterolaemia and protects from atherosclerosis development. Nat Commun. 2015;10(6):6356.
32. Le Lay S, Briand N, Blouin CM, Chateau D, Prado C, Lasnier F, et al. The lipoatrophic caveolin-1 deficient mouse model reveals autophagy in mature adipocytes. Autophagy. 2010;6(6):754–63.
33. Soussi H, Clément K, Dugail I. Adipose tissue autophagy status in obesity: Expression and flux—two faces of the picture. Autophagy. 2016;12(3):588–9.

**Figure Legends**

**Figure 1:** *Adipocyte LAL expression is decreased in obesity.*
(**A**) Adipose tissue *Lipa* mRNA expression in diet-induced murine obesity. Mice were fed control chow (n=5) or a high fat diet (n=8) for 12 weeks before mRNA extraction from subcutaneous adipose tissue. (**B**) Lipa mRNA in floating adipocytes or in cell subsets after fractionation by FACS. Four independent experiments on pooled epididymal adipose tissue digested with collagenase are shown. (**C**) *LIPA* mRNA expression in human subcutaneous adipose tissue SVF cells after collagenase digestion. Each point represents a preparation from a single donor, plotted against the BMI of the subject. The characteristics of the obese group is described in Table 1 (see group1). SVF from nine non-obese subjects (age 31.2 +/- 3.3 years, mean BMI 21.7 +/- 0.6 $Kg/m^2$) was also analyzed. No difference between lean (black dots) or obese (open dots) donors were found. (**D**) *LIPA* mRNA expression in floating adipocytes of lean or obese subjects. Only lipoaspirated subcutaneous fat tissue was available from lean subjects, whereas subcutaneous and visceral (omental) fat were collected in obese patients undergoing bariatric surgery. ** indicates statistical ($p<0.01$) difference by Mann Whitney non-parametric test. (**E**) Relationship linking subcutaneous (Sc) and Omental (Om) adipocyte *LIPA* mRNA expression in obese patients. Correlation is highly significant ($r= 0.781$, $p <0.001$). (**F**) Spearman correlations between undigested (unfragmented) adipose tissue LIPA mRNA expression and obesity-related dysfunction markers in a group of 21 massively obese patients described for clinical characteristics, indicated as group 2 in Table 1.

**Figure 2:** *Lentiviral-mediated Lipa inhibition in cultured adipocytes does not affect lysosome function or autophagic flux.*
(**A**) Efficiency of Sh sequences to inhibit *Lipa* expression in differentiated 3T3-L1 adipocytes. Three independent experiments were performed. (**B**) Impact of LAL inhibition on total cholesterol contents (free and esterified) of differentiated adipocytes maintained in standard medium, supplemented or not with 0.1mg/ml OxLDL (ThermoFisher, J65591) for 2 days. Mean values +/- sem from three independent experiments are shown, differences between groups were tested by Student's t test. (**C**) Triacylglycerol (TG) content of adipocytes assessed after lipid extraction and normalization to cell proteins. (**D**) Perilipin expression by Western blot analysis. The two perilipin isoforms were quantified and normalized to ß-actin signals. Bars represent mean values +/- sem of three independent determinations. * indicate significant differences by Student's t test. (**E**) Lysosome imaging of living adipocytes after pulse labelling for 4 hour with 0.3mg/ml 10,000MW Dextran Texas–Red (Molecular Probes, D1863) followed by 2-hours chase and fixation. Perilipin immunolabelling followed by incubation with 300nM DAPI (ThermoFicher, D3571) was included before mounting in Fluoromount-G (Sothern-Biotech, 0100-01). Red fluorescence intensity was quantified in delineated cells and normalized to surface area using image J. (**F)** Western blot analysis of LC3-II and p62 protein contents in cells exposed or not to lysosome inhibitors to assess autophagic flux. Each lane represents independently generated stably transfected population. Bafilomycin A1 (BAF, 0.1µM) or Chloroquine (CLQ, 25µM) were added for 4 hours. (**G-H**) Quantification of western blots signals after normalization to ß-actin. Values are mean +/- sem from at least three independent cell pools, each normalized to control condition with no lysosome inhibitor. **(I-K)** Lipolytic rates were determined under basal (I) or isoproterenol-stimulated conditions, in the presence or absence of Bafilomycin (BAF) to inhibit lysosomes (J-K). Experiments were repeated 3-4 times. Values are mean +/- sem.

**Figure 3:** *Stable LAL knock-down affects adipocyte cholesterol homeostasis.*
(**A**) Stratification of stable transfectants according to *Lipa* residual expression. A total of 17 independent cell pools were analyzed for *Lipa* mRNA and assigned one of the three groups by comparison with parental non transfected controls. (**B**) RT-qPCR determination of cholesterol-regulated genes mRNA in cell groups with gradual *Lipa* inhibition. Significant differences by Student t test are shown. (**C**) Spearman correlation of *Srebf2* mRNA and *Lipa* residual expression. Correlation coefficient is indicated, $p<0.05$. (**D**) Pretreatment of cells with exogenous free cholesterol to replenish intracellular pools was performed by adding 1mg/ml cholesterol (Sigma-Aldrich, C3045) in DMEM containing 1% of fatty acid free bovine serum albumin for 1-hour. Medium was removed and cells were incubated in fresh medium for subsequent 4-hours before lysis. *Hmgcr* and *Srebf2* mRNA were assessed as above. (**E**) Perilipin fluorescence intensity normalized to cell area was quantified in *Lipa* deficient cells and controls. (**F)** FAS protein content was assessed by western blot in clones with different degrees of Lipa inhibition, and normalized to ßactin. (**G)** Lipid droplet diameter measurement using PerfectImage Software (Claravision). Each point represents mean diameter values+/- sem of independent cell pools, plotted against *Lipa* residual expression. Statistically significant ($p<0.05$) negative correlation linking LAL expression and LD size is shown with correlation coefficient. ER stress markers *Grp78* (**H**) and *Atf4* (**I**) mRNA were assessed following cell incubation for 6h in serum-free medium before addition of 0.5mM Dithiothréitol (Invitrogen, D1532) for 1hour. Three independent experiments were performed, with 6 independent stable transformants in each group. Values are means+/- sem, normalized to 18S RNA.

**Figure 4:** *Validation of adipose-specific LAL overexpression in mice.*
(**A-B**) RT-qPCR expression of total LAL (endogenous plus transgenic) mRNA in adipose depots and liver of female (**A)** and male (**B**) mice. Three adipose depots: gonadal fat (Ovarian (OvAT) or Epididymal (EpiAT)), Subcutaneous (ScAT) and Brown (BAT) adipose tissues were evaluated in female and male mice of indicated genotypes. Statistical differences between genotypes by Student's t test are shown. (**C**) Linear regression plots indicating strong dependence of total LAL expression to transgenic LAL mRNA in adipose tissues of female mice. Correlation coefficients and p values are indicated for each tissue. (**D**) Body composition (**E**) Body weight gain and (**F**) adiposity of female mice fed a HFD for 12 weeks. **(G)** ScAT lipolysis was assessed *ex vivo* by measuring glycerol release from tissue fragments in the presence or not of $10^{-5}$M isoproterenol. Incubation was for 2 hours at 37°C in humidified atmosphere with 5% $CO_2$. Lipolytic activity was normalized to tissue weight.

**Figure 5:** *Metabolic phenotype of adipose-specific LAL overexpressing mice.*
(**A**) mRNA expression of inflammation markers in ovarian adipose tissue by RT-qPCR. (**B**) Fasting glycemia and (**C**) oral glucose tolerance (glucose load 2g/kg) were assessed after food withdrawal for 6 hours. * indicate differences between groups by Student's t test. (**D**) Correlation linking fasting glycemia and serum cholesterol in HFD fed mice. (**E**) Cholesterolemia and (**F**) Triglyceridemia were assessed as described in methods. **(G-H**) Indirect calorimetry was performed in HFD fed mice, maintained at room temperature. Five mice in each group were followed during five consecutive days. (**G**) Mean 24-h food intake and locomotor activity during day or night time were recorded. (**H**) Energy expenditure was

calculated from gas respiratory exchange data. (**I**) Relationship linking body weight gain during HFD and total LAL expression in BAT.

**Figure 6:** *LAL mice phenotype at thermoneutrality.*
(**A**) Preservation of genotype-dependent LAL expression in mice kept at thermoneutrality for 4 weeks. (**B**) BAT morphology in HFD mice housed at room temperature or thermoneutrality (white area are lipid droplets). **(C**) Inter-genotype comparisons of body weight changes in mice raised conventionally or housed at thermoneutrality (30°). **(D**) Body composition of mice maintained at thermoneutrality for 4 weeks on HFD. Of note, inter-genotype differences in body weight are linked to preexisting differences in lean mass but not fat. **(E)** Cholesterolemia and **(F)** glucose tolerance assessed by OGGT on HFD mice maintained at thermoneutrality for 4 weeks.

**Figure 7:** *LAL overexpression regulates BAT cholesterol homeostasis.*
After lipid extraction, BAT triglyceride (**A**), and BAT free cholesterol **(B)** were assessed in conventional mice fed HFD. inset shows unchanged min to max of esterified cholesterol values (as the difference from total to free cholesterol determinations). Significant differences by Student's t test are indicated. (**C**) BAT mRNA expression of SREBP-regulated genes, (**D**) genes related to cholesterol efflux, and UPR markers (**E**) . Statistical differences by Student's t test are indicated. (**F**) Spearman correlation linking *Ucp1* mRNA and LAL expression in BAT samples. (**G**) *Ucp1, Cidea and Dio2* mRNA were assessed in ScAT of female mice raised at room temperature (14-16 per group) and plotted as violin plots to visualize heterogeneity of individual values between groups. (**H**) BAT expression of steroidogenic genes by RT-qPCR. Significant differences by Student's t test are indicated. (**I**) Spearman correlation of *Nr5a1* mRNA expression to BAT LAL expression or body weight gain on HFD (**J**).

**Figure 8:** *Cholesterol-derived serum steroids in LAL overexpressing mice.*
Pregnenolone **(A)** 17-OHpregnenolone **(B)**, 5α-dihydrotestosterone **(C)**, and Testosterone **(D)** concentrations in mice serum were expressed as ng/ml. * indicates significant difference between groups ($p<0.05$) by Student's t test. Spearman correlations between BAT *Nr5a1* mRNA expression and serum 17-OHpregnenolone **(E)** or 5α-dihydrotestosterone **(F)**. **(G)** SREBP target genes response reflecting intracellular cholesterol gauge as a common mechanism underlying the impact of adipose LAL overexpression or knock-down in the models used in this study. In LAL overexpression, accelerated cholesterol uptake is suggested by low blood cholesterol levels. In the human situation, non-obese and obese subjects exhibit differences in adipocyte LAL expression, suggesting potential benefice in therapeutical LAL activation.

**Table 1**: **Clinical characteristics of obese patients**

| | **Group 1 (n=45)** | | **Group 2 (n=21)** | |
|---|---|---|---|---|
| | **mean** | **sem** | **mean** | **sem** |
| Age (Years) | 45.4 | 2.16 | 45.7 | 3.04 |
| BMI Kg/M2 | 47.22 | 1.30 | 46.88 | 1.90 |
| Fat Mass % | 49.64 | 0.57 | 48.96 | 0.88 |
| Fasting glucose (mM) | 6.11 | 0.28 | 5.72 | 0.28 |
| Fasting Insullin (µUI/ml) | 21.44 | 2.17 | 25.13 | 3.25 |

| | | | | |
|---|---|---|---|---|
| HbA1c (%) | 6.47 | 0.21 | 6.105 | 0.21 |
| Cholesterolemia (mM) | 4.11 | 0.24 | 4.63 | 0.24 |
| Triglyceridemia (mM) | 1.64 | 0.14 | 1.71 | 0.22 |
| HDL Cholesterol (mM) | 1.15 | 0.05 | 1.04 | 0.07 |
| ASAT (IU/l) | 30.94 | 2.95 | 29.47 | 4.76 |
| ALAT (IU/l) | 35.67 | 7.30 | 41.11 | 14.59 |
| GGT (mg/dl) | 46.1 | 7.34 | 46.40 | 12.00 |
| Leptinemia (ng/ml) | 73.8 | 6.50 | 85.16 | 11.39 |
| Adiponectinemia (µg/ml) | 4.07 | 0.30 | 4.23 | 0.32 |
| IL6 (pg/ml) | 5.08 | 0.53 | 4.48 | 0.48 |

Group 1: AT samples were directly frozen and used for LIPA mRNA expression in unfractionated adipose tissue.
Group 2: Freshly collected AT samples were digested with collagenase to separate isolated adipocytes and stroma vascular cell fractions for further investigation of the topology of LIPA expression in cell subfracti0ns.

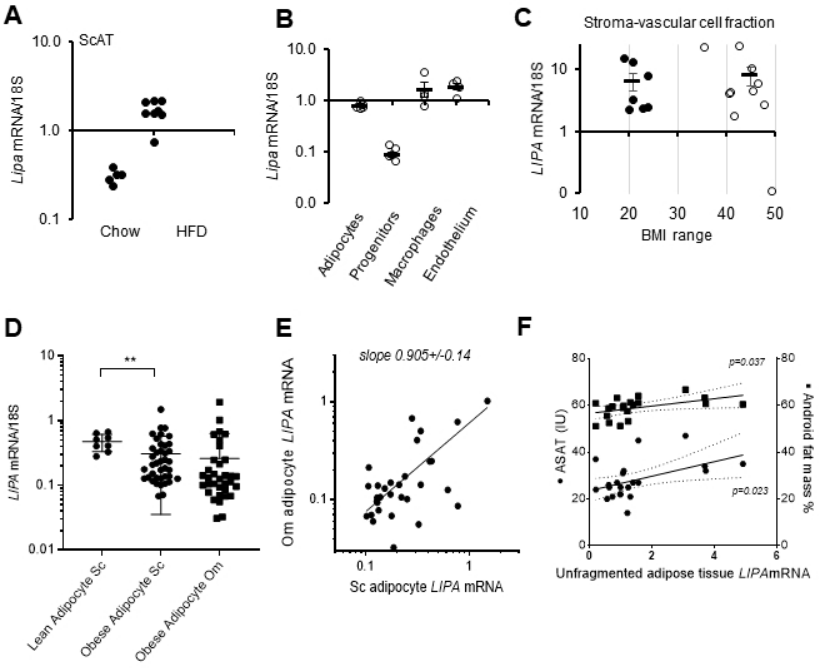


Figure 1

Figure 1

190x254mm (96 x 96 DPI)

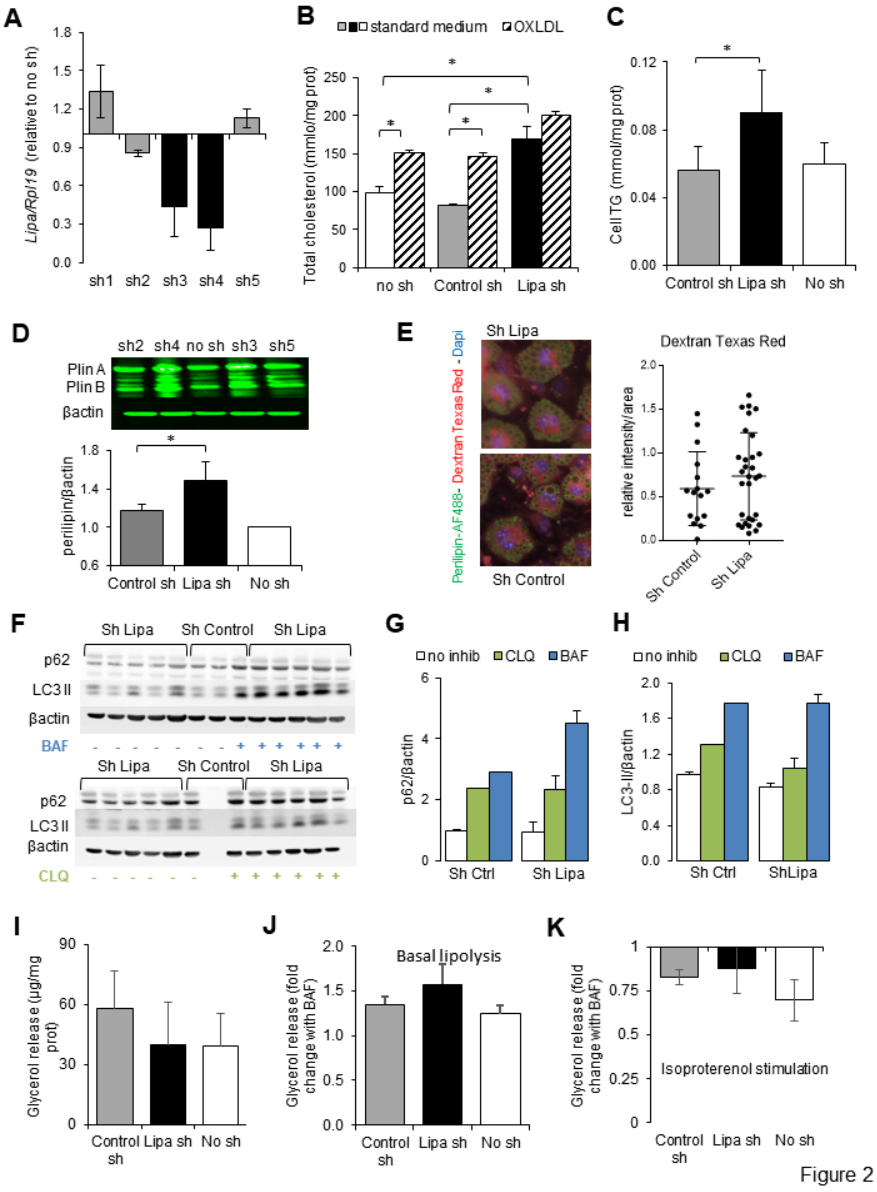


Figure 2

Figure 2

190x254mm (96 x 96 DPI)

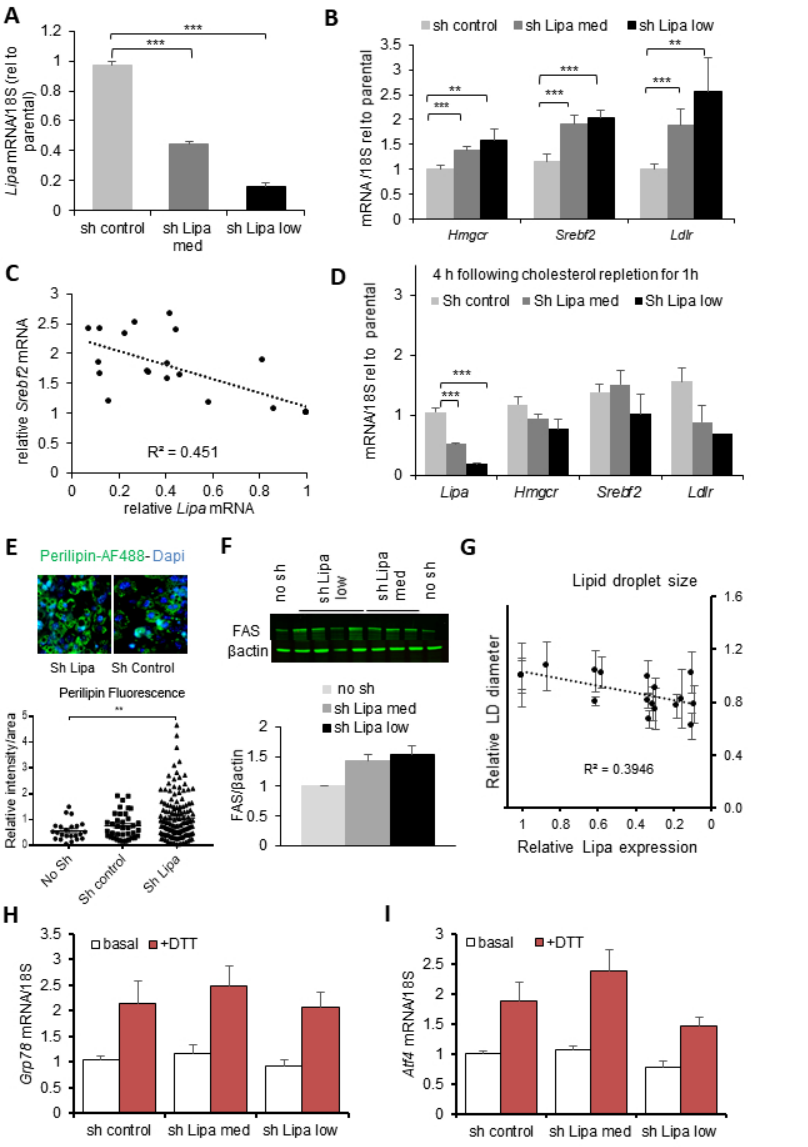


Figure 3

Figure 3

190x254mm (96 x 96 DPI)

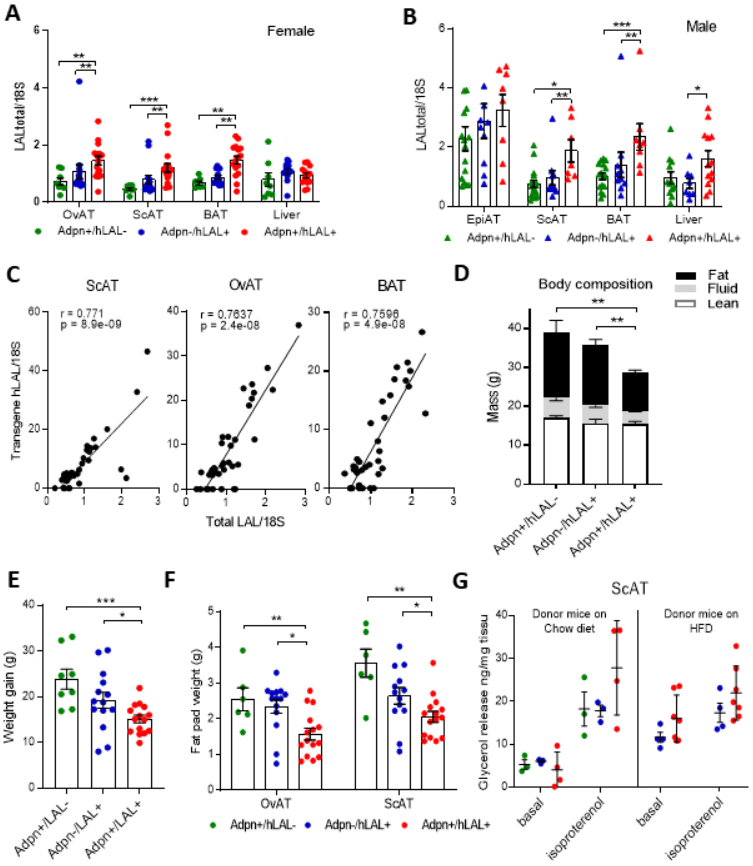


Figure 4

Figure 4

190x254mm (96 x 96 DPI)

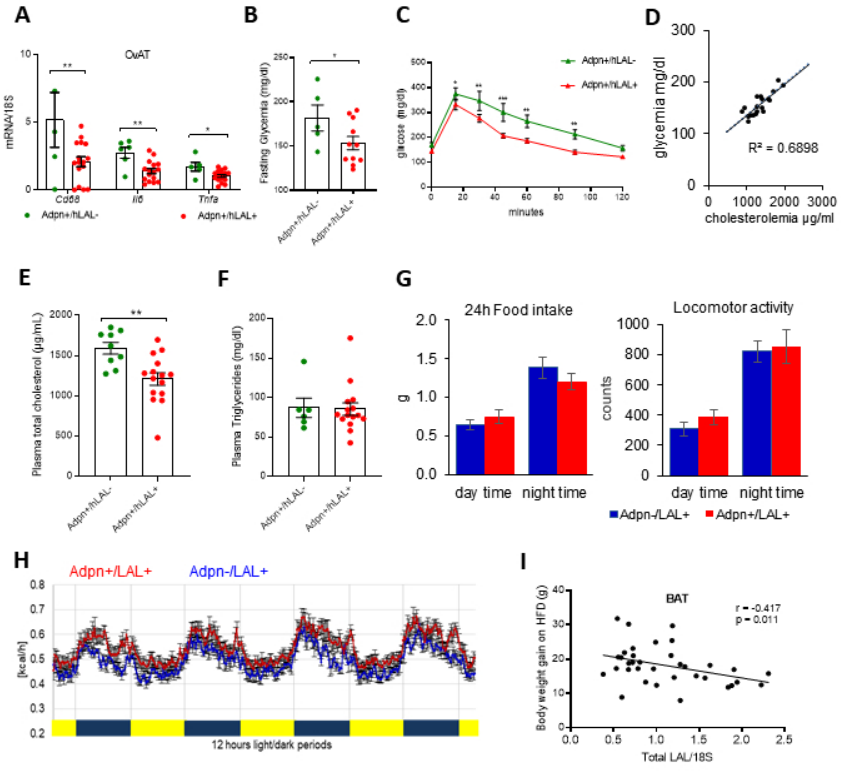


Figure 5

Figure 5

190x254mm (96 x 96 DPI)

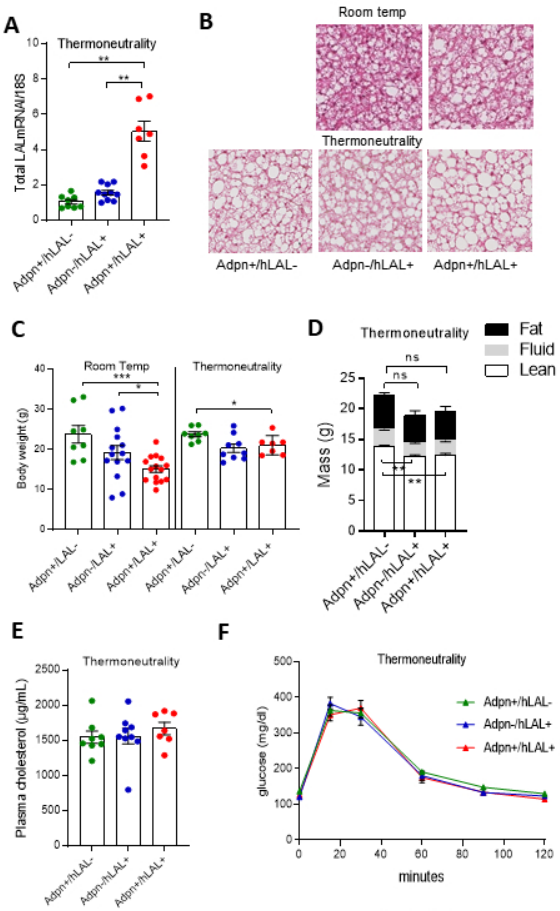


Figure 6

Figure 6

190x254mm (96 x 96 DPI)

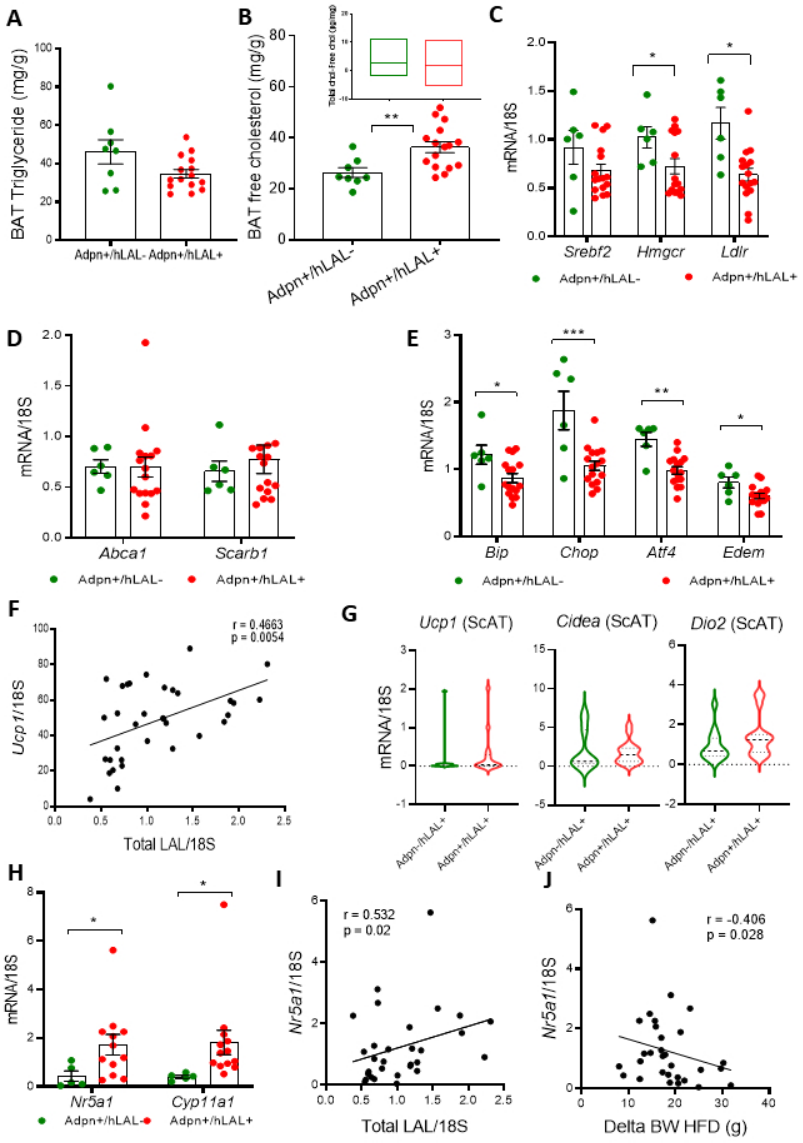


Figure 7

Figure 7

190x254mm (96 x 96 DPI)

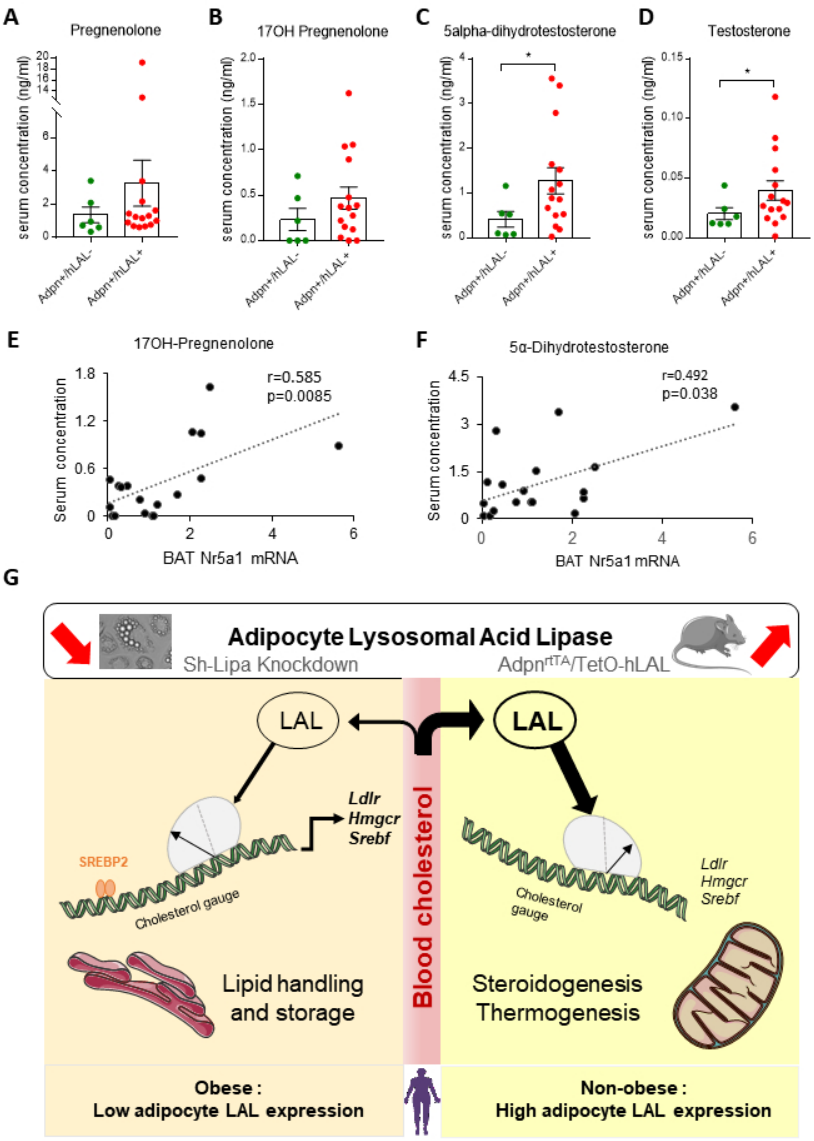


Figure 8

Figure 8

190x254mm (96 x 96 DPI)

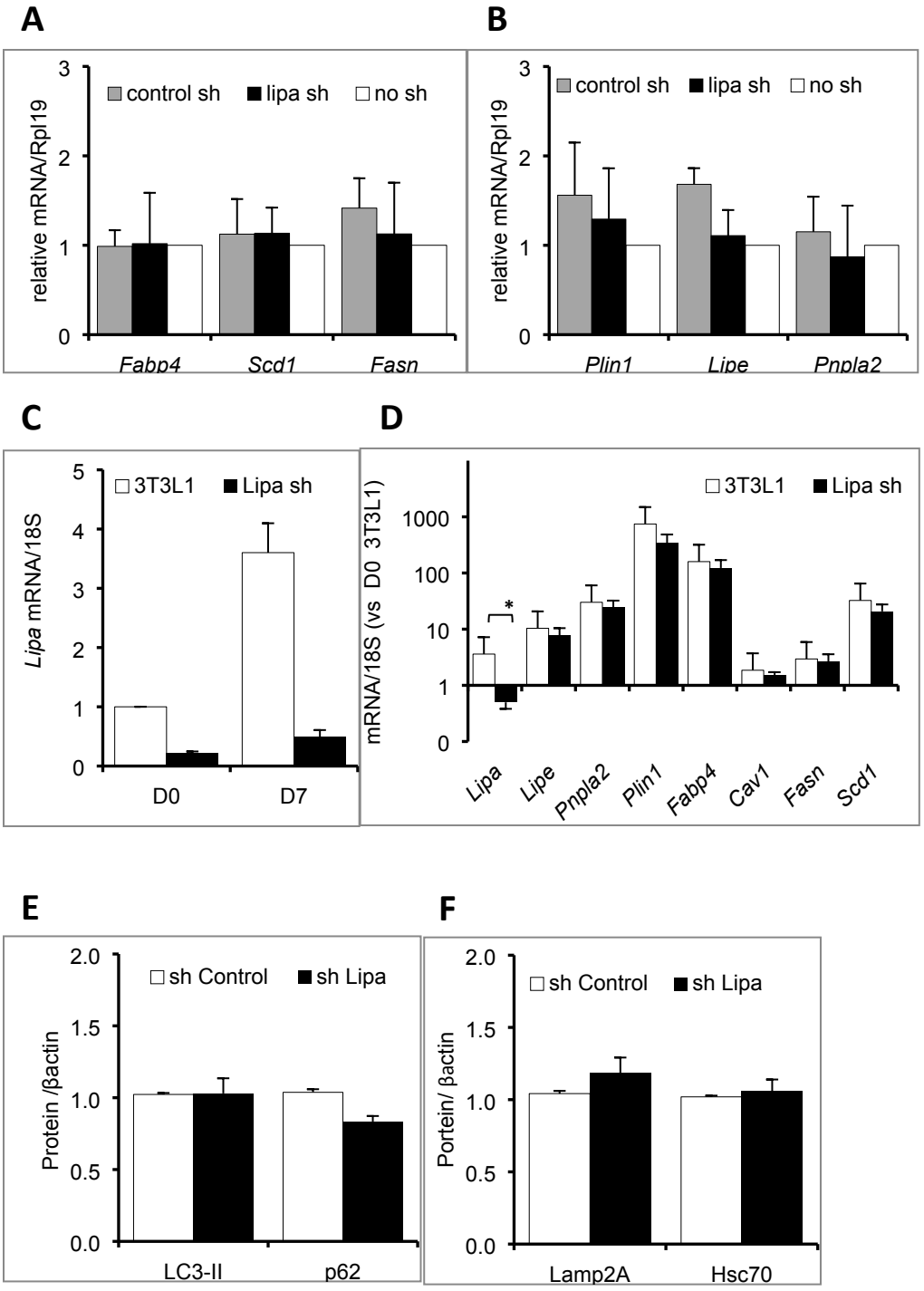


**Supplemental figure 1:** *Impact of Lipa Knockdown in cultured adipocytes.*
(**A-B**) Impact of *Lipa* inhibition on adipocyte gene expression. mRNA encoding major adipocyte lipases (**A**) or lipid storage genes (**B**) assessed by RT-qPCR.
(**C-D**) Stable *Lipa* inhibition in preadipocytes (D0) or differentiated fat cells (D7) after puromycin selection. (**D**) Adipose differentiation is unaffected by *Lipa* inhibition. mRNA was extracted from independently generated sh-knock-down or parental cells in the fully differentiated state (D7). For each gene, mRNA levels in the parental 3T3-L1 undifferentiated cells were arbitrary set to 1. Western blot analysis of cell protein contents for autophagic effectors **(E)**, or Lysosomal chaperones **(F)**. Values are means +/- sem of 5 independent cell preparations in each group.

Supplemental figure 1

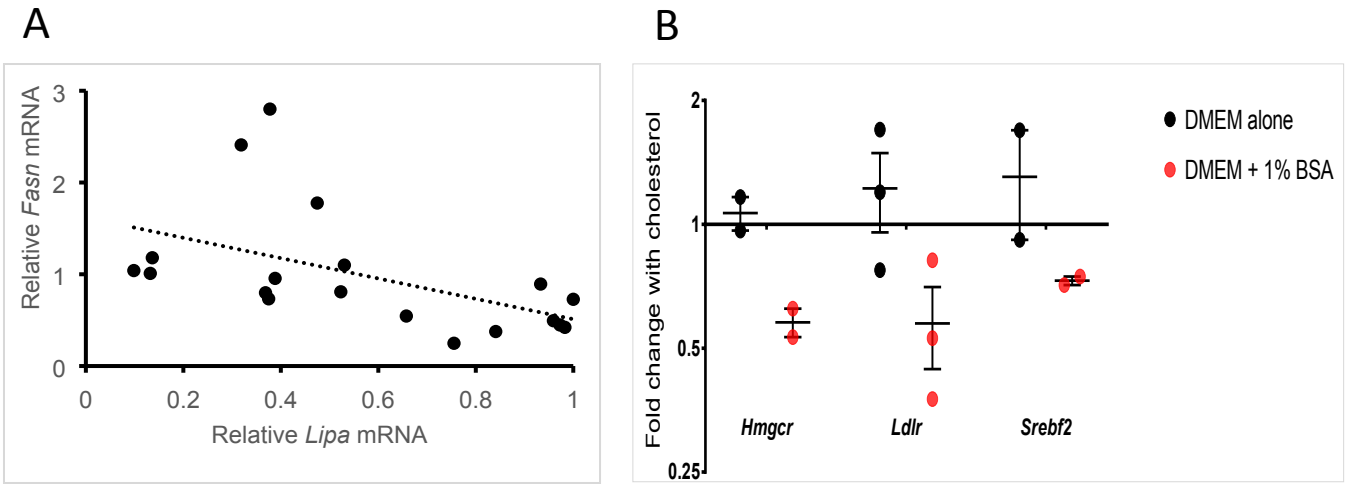


**Supplemental figure 2***:*
**A.** *Correlation between Lipa expression and Fasn* in differentiated cells with different degrees of Lipa inhibition.
**B.** *Down-regulation of SREPB2 target genes after 1 hour of incubation with exogenous cholesterol*. Cholesterol was supplied as an ethanol solution (1mg/ml final concentration) in DMEM containing or not 1% of fatty acid-free bovine serum albumin. Down regulation is seen only when a protein acceptor is present in the medium. 2-3 independent determinations were performed on control 3T3-L1 cell batches.

Supplemental figure 2

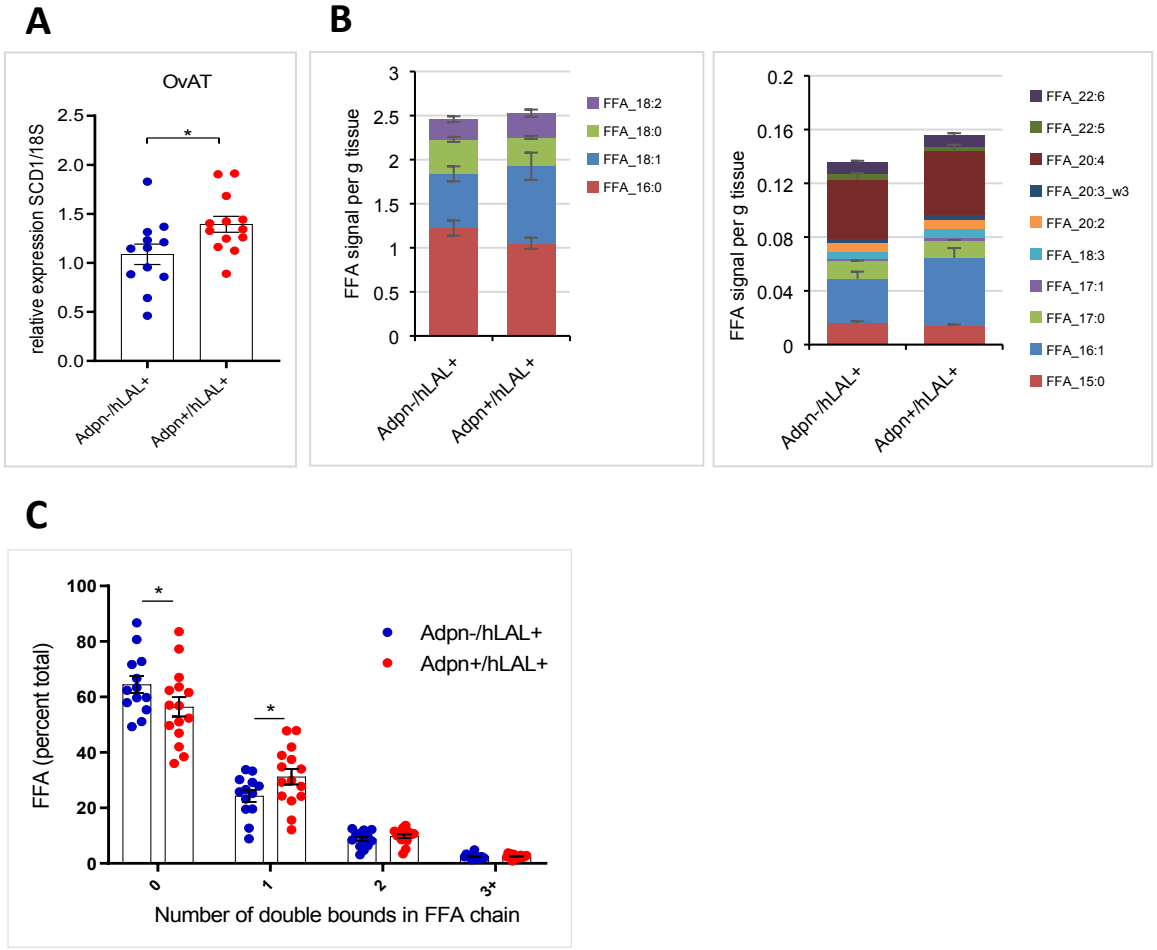


**Supplemental figure 3:** I*mpact of Adipose LAL overexpression on tissue free fatty acid profiles. (***A***) Scd1* fatty acid desaturase mRNA levels in OvAT. (**B**) Free fatty acid profiles were quantified by GC/MS after extraction with isooctane and *derivatization with* pentafluorobenzyl bromide.13 individual fatty acid species that could be detected in OvAT adipose tissue extracts. (**C)** Changes in the proportion of monounsaturated versus saturated fatty acid ratios were found in LAL overexpressing adipose tissue. * indicates a significant difference by Student's t test.

Supplemental figure 3

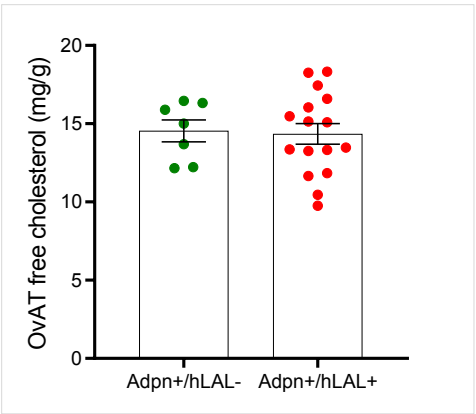


**Supplemental figure 4:** Free cholesterol contents in white (OvAT) adipose tissue.

Supplemental figure 4

# Lysosomal acid lipase drives adipocyte cholesterol homeostasis and modulates lipid storage in obesity, independent of autophagy.

Camille Gamblin[1], Christine Rouault[1], Amélie Lacombe[2], Francina Langa-Vives[4], Dominique Farabos[5], Antonin Lamaziere[5], Karine Clément[1], Emmanuel L. Gautier[2], Laurent Yvan-Charvet[3], Isabelle Dugail[1].

[1] UMRS 1269 Inserm/Sorbonne University, Nutriomics, Paris, France
[2] UMRS 1166 Inserm/Sorbonne University, Paris, France
[3] UMRS 1065 Inserm/ Nice Sophia Antipolis University, C3M, Nice, France
[4] Mouse Genetics Engineering Center, Pasteur Institute ~~Pasteur~~, Paris, France
[5] Sorbonne University INSERM, Saint Antoine Research center, CRSA, INSERM, Département de Métabolomique Clinique, Hôpital Saint Antoine, AP-HP/Sorbonne Université, Paris, France

Corresponding author: Isabelle.dugail@inserm.fr

Short running title: LAL in adipocyte cholesterol homeostasis

Word count: 3995. References: 33. Figures: ~~7.~~8 Table: 1.

Abstract

Besides cytoplasmic lipase-dependent adipocyte fat mobilization, the metabolic role of lysosomal acid lipase (LAL), highly expressed in adipocytes is unclear. We show that the isolated adipocyte fraction but not the total undigested adipose tissue from obese patients has decreased LAL expression compared to non-obese. Lentiviral-mediated LAL knockdown in 3T3L1 to mimic obese adipocytes condition did not affect lysosome density or autophagic flux, but increased triglyceride storage and disrupted ER cholesterol as indicated by activated SREBP ~~tone~~. Conversely, mice with adipose-specific LAL overexpression (Adpn-rtTA x TetO-hLAL) gained less weight and body fat than controls on a high fat diet, resulting in ameliorated glucose tolerance. Blood cholesterol was lower than controls albeit similar triglyceridemia. Adipose-LAL overexpressing mice phenotype is dependent on the housing temperature, and develops only under mild hypothermic stress (room temperature) but not at thermoneutrality (30°C), demonstrating prominent contribution of BAT thermogenesis. LAL overexpression increased BAT free cholesterol, decreased ~~attenuated~~ SREBP targets~~tone~~, and induced the expression of genes involved in initial steps of mitochondrial steroidogenesis, suggesting conversion of lysosome-derived cholesterol to pregnenolone. In conclusion, our study demonstrates that adipose LAL drives tissue cholesterol homeostasis and impacts BAT metabolism, suggesting beneficial LAL activation in anti-obesity approaches aimed at reactivating thermogenic energy expenditure.

## Introduction

Lysosomal acid lipase (Lipa or LAL) is the sole non-polar lipid esterase within lysosomes. Due to human gene mutations, partial inactivation of LAL (as in cholesterol storage disease) or total absence~~inactivity~~ (as in Wolman syndrome) promote ectopic lipid accumulation, hyperlipemia, inflammation and multi-organ (particularly liver) failure (1). According to substrate specificity and pH spectrum, LAL is involved in the utilization of exogenous lipids that enter through receptor-mediated endocytic pathway. As such, LAL regulates macrophage inflammation downstream of lipoproteins endocytosis and efferocytic clearance of apoptotic bodies (2). It is also part of the gene program driving the metabolic switch ~~–~~from a glucose utilizing proinflammatory M1-like macrophage toward a M2-like lipid oxidizing phenotype that promotes tissue remodeling (3). More globally, GWAS analysis of gene variation ~~in GWAS~~ identified LAL as a susceptibility locus for cardiovascular disease (4), suggesting a role in metabolic regulation.

In the context of diabetes and metabolic diseases, interest in lysosomal lipid hydrolysis has raised following the discovery of lipophagy (5), a LAL-dependent autophagic process for cytoplasmic lipid droplets in which lysosomes ultimately break down triglycerides (TG). Indeed, lipophagy is now recognized a critical step in the control of ~~lipid engorgement in~~ hepatocyte steatosis, and selective inhibition of liver autophagy produces fatty liver disease in mice (6). It is now recognized that hypothalamic neurons (7) and macrophages (8) also degrade their TG stores by lipophagy, highlighting preference for acid versus neutral lipolysis in some cell types. Adipocytes, which respond to nutritional inputs by orchestrating lipid mobilization and fatty acid fluxes across the body are essential to maintain metabolic health. Adipose tissue is equipped with highly regulated cytoplasmic lipases that become activated at the lipid droplet surface to fine tune lipid release (9)(10). Despite well-established importance of adipose tissue cytoplasmic lipolysis, high LAL expression is also found in fat cells, which suggests additional roles besides triglyceride mobilization.

Starting from the observation of a decreased adipocyte LAL expression in human obesity, we have investigated the impact of LAL gain and loss of function in cultured fat cells and in mice, which highlights an inverse relationship to adipocyte storage, linked to reorientation of fat cell cholesterol metabolism and thermogenesis, independent of lipophagy. Altogether, our data present an extensive analysis of the impacts of adipocyte LAL modulation, and reveal beneficial metabolic effects of LAL stimulation through cholesterol dynamics.

## Research Design and Methods

*Human adipose tissues*- Subcutaneous adipose tissue from periumbilical region or omentum were excised from obese patients during bariatric surgery at La Pitié-Salpétriere Hospital (Paris), in accordance with local Ethical Committee recommendations (0811792). All participants provided written informed consent. Clinical description (Table1) is provided for two groups according to adipose samples use: direct congelation (group 1, n=45) or collagenase treatment (group 2, n=21). Periumbilical adipose tissue from eight non-obese healthy subjects was obtained by lipoaspiration (Clinique Remusat, Paris, France).

*Sh-mediated LAL downregulation* – 3T3-L1 cells were induced to differentiation with Dexamethasone 1.25µM (Sigma-Aldrich, D1756), IBMX 250µM (Sigma-Aldrich, 15879), Insulin 250nM (Sigma-Aldrich, 19278) for three days followed by insulin alone. 3T3-L1 were transduced with different lentiviral sh vectors (Sigma-Aldrich, 1-TRCN000076829, 2-TRCN000076831, 3-TRCN000076832, 4-TRCN000288217, 5-TRCN000295618) when fully differentiated or as undifferentiated preadipocytes, subsequently selected with puromycin (ThermoFisher, A1113802) to establish stable cell lines

*Autophagic flux* - Cultured cells were serum-starved for 6h before addition or not of lysosome inhibitors: 0.1µM BafilomycinA1 (Sigma-Aldrich, B1793), or 25µM Chloroquine (Sigma-Aldrich, C6628) for 4 hours. P62 and LC3-II were probed by western blotting.

*LAL mouse lines* – TetO-CMV-hLAL mice were obtained by additive transgenesis (Pasteur institute, Paris) by injecting into C57/Bl6J embryos a TRE-CMV promotor upstream of hLAL cDNA, purified from a pTRE2hyg plasmid. Adipose-specific LAL overexpressing mice were generated by breeding Adpn-rtTa mice with TetO-CMV-hLAL and genotyping with 5'-AGCCCAGTGTAAAGTGGCCC-3' 5'-CTGGACAAGAGCAAAGTCAT-3' and 5'-TGTGCCTTAACCGAATTCCT-3' 5'-CTGGTTTGGGACCTTTGTCA-3'. Weaned littermates were fed HFD (Research Diet, D12492i) with free access to drinking water containing 1g/L Doxycycline (Sigma-Aldrich, D9891).

*Mice phenotyping* – Mice were housed at room temperature (22°C) or thermoneutrality (30°C) in a climate chamber (TSE, PhenoMaster). Body composition was analyzed by nuclear magnetic resonance (Bruker Mouse Minispec, LF90). Blood and fat pads (gonadal (OvAT-EpiAT), subcutaneous (ScAT), brown adipose tissue (BAT)) were frozen in liquid nitrogen or fixed with Formalin (Sigma Aldrich, HT501128), or incubated with collagenase as described (11). Oral glucose tolerance test (OGTT) started by gavage with 2.0 g/kg glucose in mice fasted for 6h. Glycemia was followed with a sugar test meter (ACCU-CHECK, Roche). Serum steroid profiling was measured by LC/MS-MS according to established methods (12)

*Indirect calorimetry* – Mice were acclimated in individual cages for 2 days before measurement of $VO_2$, $VCO_2$, locomotor activity, food and water consumption over 5 consecutive days at 22°C (PhenoMaster, TSE). HFD and Doxycycline were maintained.

*Gene and Protein expression* - Total RNA was extracted using an RNeasy Mini kit (Qiagen, 74104), followed by Quantitative real-time PCR using Master Mix (Applied Biosystems). Lysates in RIPA buffer (Sigma Aldrich, R0278) containing proteinase inhibitors (Complete Mini, Roche) were prepared (Bertin Technologies, Precellys 24) and cleared for 10min at 10.000rpm. Protein concentration was measured (ThermoFisher Scientific, BCA assay). western blotting was performed as described (13).

*Adipose tissue lipolysis — Cultured adipocytes or* ScAT fragments were incubated into DMEM containing 1% bovine Serum Albumin (Sigma-Aldrich, A8806) for 2h at 37°C with or without 10µM Isoproterenol (Sigma-Aldrich, 1351005). Released glycerol was measured with Free Glycerol reagent (Sigma-Aldrich, F6428). Frozen tissues were used to determine cholesterol (Amplex red kit, Invitrogen, A12216) or triglyceride (Cayman, 10010303) contents.

*Statistical Analysis - U*npaired two-tailed t tests, ANOVA analysis, Mann Whitney non-parametric tests or Spearman correlations were performed with GraphPad Prism 7.

*Data and resources availability* - TetO-CMV-hLAL mouse strain generated during the current study is available from the corresponding author upon request.

**Results**

*Decreased adipocyte -but not whole adipose tissue- LAL expression in human obesity.*

Adipose tissue LAL expression is poorly documented. In mice, positive association to body weight was reported, with elevated *Lipa* mRNA in obese compared to lean fat pads (14). In agreement, we have observed increased Lipa mRNA in the fat tissue of mice made obese by high fat diet feeding compared to lean animals fed chow *(Figure 1A)*. Moreover, microarray analysis of human subcutaneous adipose tissue LIPA expression replicated on 2 independent groups of obese (BMI>30Kg/m2) compared to non-obese subjects (BMI<30Kg/m2) indicated significantly upregulated LIPA signal in obese patients (fold change 1.55 and 1.07; q value 0.031 and 0.005 respectively). To pinpoint the origin of this regulation, we first analyzed *Lipa*

expression in the main cell sub-populations comprised in mice adipose tissue i.e. ~~. Compared to isolated mature adipocytes, high levels of *Lipa* mRNA were found in the stroma-vascular fraction (SVF) that includes all non-adipose cell types within fat tissue (Figure 1A). Further, among~~ mature adipocytes or the different cell types in SVF separated by FACs as previously described ~~in~~ (15)~~.~~; W~~ w~~e observed comparable *Lipa* expression in floating adipocytes, endothelial cells ($Cd45^-Cd31^+$)~~,~~ and resident macrophages ($Cd45^+$ $F4/80^+$), but very low mRNA levels in progenitor cells defined as $Cd45^-Cd31^-Cd140^+$ *(Figure 1B)*. This suggested that cell composition, especially the adipose versus non-adipose cell ratio might be a strong determinant of tissue LAL expression. In ~~subcutaneous fat of~~ non-obese subjects or patients with massive obesity (mean BMI 47 $Kg/m^2$, Table 1) SVF LIPA mRNA was independent of the BMI of the donor on a per cell basis *(Figure 1C)*. This suggested that ~~previously reported~~ up-regulation of LAL expression with obesity is linked to the number of stromal cells present in fat, especially infiltrated macrophages. Importantly, contrary to stromal LAL, obesity modulated floating adipocyte expression, and LIPA mRNA was lower in obese compared to lean adipocytes *(Figure 1D)*. Within the bariatric obese cohort in which two distinct fat tissue depots (subcutaneous and omental) could be sampled in the same patient, adipocyte LIPA mRNA was highly concordant between fat locations *(Figure 1E)*. Unfractionated adipose tissue biopsies, available in a separate group of obese patients with very similar characteristics *(Table 1)* did not revealed links between LIPA expression and indicators of obesity severity (body weight, BMI or total fat mass), but showed positive correlation with markers of ~~between LIPA mRNA and~~ obesity-related dysfunction ~~markers~~ such as android fat distribution or circulating ASAT *(Figure 1F)*. These findings indicate that total adipose tissue LAL is a ~~stronger~~ marker of metabolic impairment in obesity, rather than an indicator of obesity severity~~fat mass per se~~. Thus, these experiments reveal a complex pattern of obesity-related adipose LAL regulation, with a strong dependence on tissue composition with regard to non-adipose cells, ~~which coexist~~concomitants~~s~~ with a deficit of LAL expression in mature adipocytes. They highlight the need for cell type-specific studies to address the question of the significance of adipocyte LAL.

*Adipocyte LAL down-regulation by lentiviral shRNA promotes fat accumulation and affects lipid droplet dynamics, independent of autophagy.*

To explore the consequences of obesity-linked adipocyte LAL down-regulation ~~in obesity~~, we modulated LAL expression using lentiviral vectors to reduce LAL in fully differentiated lipid-laden 3T3-L1 cells, a recognized model for fat cells. Five days after differentiation, when clearly visible lipid droplets had accumulated, cells were transduced with five different sh lentiviral stocks or no virus, and LAL expression was assessed after additional 7days. Among five sequences, two (sh3 and sh4) inhibited LAL expression with more than 50% efficiency, whereas the other three (sh1-2-5) showed slight or no inhibition *(Figure 2A)*. Cells treated with sh3-4 were analyzed together and thereafter denominated Lipa sh, whereas cells treated with inactive sh1-2-5 were considered sh controls. Similar to that reported in genetically or pharmacologically LAL-deficient macrophages (16) adipocyte LAL down-regulation raised ~~led to~~ total cholesterol cell content~~accumulations~~ *(Figure 2B)*. Further, high doses of oxidized LDL (Ox-LDL), known to inhibit LAL activity (17)~~,~~ increased cholesterol contents in LAL expressing adipocytes ~~(no sh group: x1.5, control sh: x1.8)~~ up to the level of Lipa Sh cells *(Figure 2B)*. Thus, ~~cholesterol loading~~ as a hallmark of LAL functional impairment cholesterol loading is seen in both OxLDL treatment and lentivirus-mediated *Lipa* knockdown.

Not only cholesterol esters but also TG are LAL substrates. Despite unaffected expression of cytoplasmic lipases and~~,~~ lipid droplet-coating *Plin1 (Supplemental Figure 1A)*, or adipocyte specific ~~lipogenic~~ genes *(Supplemental Figure 1B)*, we found that TG contents were higher in

Lipa sh cells compared to control sh or untransfected cells *(Figure 2C)*. Perilipin1 protein content increased in Lipa sh compared to controls *(Figure 2D)*, further indicating lipid droplet accumulation. Thus, LAL down-regulation favors adipocyte TG storage.

We next generated stable shRNA *Lipa* knock-down by puromycin selection, in which low levels of LAL mRNA were maintained before (D0) or after (D7) full differentiation ~~were present~~ *(Supplemental Figure 1C)*. Overall fat cell conversion was unaffected, as indicated by normal adipocyte markers expression *(Supplemental Figure 1D)*. Lysosome integrity and density was conserved as shown by protein contents of lysosome chaperones ~~(~~Lamp2A and Hsc70~~)~~ *(Supplemental figure 1E)* and pulse-chase labeling with Dextran-Texas Red *(Figure 2E)*. Autophagosome marker (LC3-II) or autophagic substrate (p62) contents were also similar in control and LAL-deficient cells *(Supplemental figure 1F~~not shown~~)*. Treatment with lysosome inhibitors (Chloroquine (CQ) and BafilomycinA1 (BAF)) to assess autophagic flux showed equivalent accumulation rates of p62 and LC3-II *(Figure 2F-H)*, indicating unaffected lysosomal clearance in LAL-deficient conditions. Regarding lipolysis, the presence of BAF did not affected basal glycerol release, which was also not different in LAL deficient and in controls (*Figure 2I-J*). BAF only slightly inhibited isoproterenol-stimulated lipolysis by less than 25% in control adipocytes (*Figure 2K* and previous data (12)), an effect that was also found in LAL deficient cells (*Figure 2K*), suggesting a lipophagy-unrelated action. Of note, lysosome inhibitors did not affect Perilipin1 contents (not shown), indicating that the adipocyte-specific isoform is not degraded in lysosomes, contrary to that shown for non-adipose perilipin-2 and -3 (18). Thus, the impact of LAL downregulation in adipocytes is ~~mostly~~ autophagy-independent.

We next investigated potential changes in cell cholesterol homeostasis, revealed by Sterol Regulatory Element Binding Protein status. As a cholesterol-regulated transcription factor, auto-regulated SREBP2 and its target genes (HMG-CoA reductase, LDL receptor~~, and SREBP2~~) are induced in response to cholesterol depletion sensed in the endoplasmic reticulum (ER). Independently generated stable transfectants were stratified into 3 groups based on residual levels of *Lipa* expression *(Figure 3A)*, in which *Hmgcr*, *Srebf2* and *Ldlr* mRNA levels gradually increased with stronger LAL knockdown, suggesting a state of ER-sensed cholesterol depletion in LAL deficiency *(Figure 3B)*. Indeed, residual *Lipa* expression negatively correlated with *Srebf2* gene expression, the lower *Lipa* mRNA, the higher *Srebf2* *(Figure 3C)*, and also varied inversely to *Fasn,* a SREBP-regulated lipogenic gene (*Supplemental figure 2A*).~~.~~ Cell replenishment with a bolus of a free cholesterol supplemented medium, followed by a 4-hour chase in standard medium was sufficient to abolish differences in *Srebf2* and *Hmgcr* mRNA between *Lipa* groups (*Figure 3D*, *Supplemental figure 2B*), suggesting that restrained LAL-dependent free cholesterol delivery to the ER was most likely the cause of upregulated expression of cholesterol-regulated genes.

As cholesterol-sensitive ER is also the site of lipid droplet (LD) assembly and budding, we probed for altered topology of TG accumulation by LAL deficiency. Concomitant with elevated TG contents and LD-associated perilipin fluorescence in Sh Lipa compared to Sh controls *(Figure 3E~~-F~~)*, we also found increased FAS protein contents in Lipa deficient cells, indicative of active lipogenesis (*Figure 3F*). ~~we u~~Unexpectedly ~~found that~~ the mean diameter of LDs proportionally declined with *Lipa* inhibition. ANOVA analysis of more than 10.000 single LDs from independent cell pools indicated significant negative contribution of LAL deficiency to LD size *(Figure 3G)*. This infers that the number of LD per cell increases in LAL deficient adipocytes, as more lipid were accommodated in smaller LDs. However, because LDs are so numerous and heterogeneous in differentiated 3T3-L1 adipocytes, direct measure of the total number of LDs per cell requires 3D reconstitution of images, difficult to accurately analyze in a sufficient number of cells. Although not directly evaluated, we~~, and also~~ suggest~~s~~ that an

increased in the number of LDs could be linked to facilitated LD budding from cholesterol-depleted ER. ~~has facilitated ability for LD budding.~~ Other ER functions, such as the UPR (Unfolded Protein Response) remained unaffected by LAL deficiency, as a normal response to an UPR inducer (Dithiothreitol) which disrupts oxidative protein folding in the ER lumen, was mounted irrespective of *Lipa* expression *(Figure 3H-I)*. Together, these data underline LAL-dependence of a specific cholesterol lysosome to ER axis in regulating adipocyte homeostasis. We propose that defective cholesterol esters hydrolysis in LAL deficit could limit free cholesterol exit from lysosomes, and induce a chronic state of cholesterol demand in the ER, in favor of LD budding.

*Adipocyte LAL overexpression in mice alleviates high fat diet induced obesity and metabolic complications.*

We next generated mice with adipocyte-specific LAL overexpression to investigate the impact of adipocyte LAL modulation at whole-body level. We bred Adpn-rtTA mice with TetO-CMV-hLAL, and fed littermates on a high fat diet (HFD) for 12 weeks with free access to doxycycline-supplemented drinking water (1g/l). We used primers recognizing both the hLAL transgene and the endogenous mouse *Lipa* mRNA~~s~~ to confirm significant over-expression of LAL in adipose tissues *(Figure 4A)*. Compared to control single transgenics (*Adpn$^{+}$/LAL$^{-}$* or *Adpn$^{-}$/LAL$^{+}$*) a significant increase in LAL expression was seen in *Adpn$^{+}$/LAL$^{+}$* female adipose tissues ~~as expected,~~ but not in the liver, as expected. In males, due to high levels of endogenous LAL in the epididymal fat (EpiAT), overexpression was seen only in brown (BAT) and subcutaneous (ScAT) depots *(Figure 4B)*. *Adpn$^{+}$/LAL$^{+}$* livers of male mice expressed unpredicted high LAL mRNA compared to controls. Thus, considering sex-specific responses, we decided to limit analysis to female only, in which transgene-driven adipocyte LAL expression was robust and consistent *(Figure 4C)*.

LAL overexpressing *Adpn$^{+}$/LAL$^{+}$* female mice gained less weight than *Adpn$^{-}$/LAL$^{+}$* or *Adpn$^{+}$/LAL$^{-}$* controls on a 12-weeks HFD *(Figure 4D)*. Analysis of body composition indicated decreased fat mass, but not lean mass or fluids *(Figure 4E)*, and less developed OvAT and ScAT depots *(Figure 4F)*. Because LAL has ~~is also a~~ TG lipase activity, we checked for stimulation of adipocyte TG mobilization to explain lower fat deposition. Basal glycerol release by *ex vivo* ScAT fragments was similar regardless the donor mice genotype or diet (chow diet or HFD). Maximally stimulated lipolysis with isoproterenol was also unaffected *(Figure 4G)*. Thus, the lean phenotype of LAL overexpressing mice is unrelated to adipocyte lipolysis and TG mobilization.

In line with their lower fat mass, LAL overexpressing mice were also less prone to HFD-dependent visceral adipose tissue inflammation and expressed less *Cd68*, *Il6* and *Tnfa* mRNA than controls *(Figure 5A)*. We also found elevated *Scd1* (StearoylCoa desaturase1) mRNA expression in the OvAT of *Adpn$^{+}$/LAL$^{+}$* mice *(Supplemental f~~F~~igure 3~~2~~A)*, which translated into a greater proportion of monounsaturated fatty acids at the expense of saturated fatty acids *(Supplemental Figure 3~~2~~B-C)*. High ratio of monounsaturated over saturated fatty acids is metabolically beneficial, as well as low adipose tissue inflammation, which prompted us to check glucose homeostasis in LAL overexpressing mice. Compared to controls, *Adpn$^{+}$/LAL$^{+}$* mice had lower fasting blood glucose *(Figure 5B)*, and their glycemic response to an oral glucose load (OGTT) was less *(Figure 5C)*. Noticeably, a highly significant correlation between glycemia and circulating cholesterol concentrations was found *(Figure 5D)*, and *Adpn$^{+}$/LAL$^{+}$* mice had lower blood cholesterol than controls *(Figure 5E)* despite comparable triglyceridemia *(Figure 5F)*. All together, these data indicate a beneficial impact of adipocyte LAL overexpression to damper the deleterious metabolic consequences of HFD.

*Improvement of metabolic response in adipocyte LAL overexpression is linked to thermogenesis.*

To investigate the cause of LAL-mediated obesity resistance upon HFD feeding in mice, we assessed energy balance components by indirect calorimetry. We explored~~investigated~~ *Adpn⁺/LAL⁺* mice against *Adpn⁻/LAL⁺* controls, and found similar food intake and locomotor activity in the two groups *(Figure 5G)* but energy expenditure profiles in *Adpn⁺/LAL⁺* were above controls *(Figure 5H)*. This suggested a role for~~of~~ thermogenesis, a prominent energy expense module required to defend mice core temperature in standard housing conditions (22°C). LAL expression in BAT inversely correlated with body weight response to HFD *(Figure 5I)*, which further suggests BAT contribution. To decipher the role of BAT-related thermogenesis in the obesity-resistant phenotype of LAL overexpressing mice, we reevaluated mice fed a HFD as above, but housed under thermoneutral conditions (i.e. 30°C instead of 22°C) to shut-off thermogenic response. LAL overexpression persisted in thermoneutrally housed *Adpn⁺/LAL⁺ mice (Figure 6A)* and BAT morphology showed expected differential lipid accumulation after 4 weeks of conventional versus thermoneutral housing *(Figure 6B)*. Within this 4-week period, we did not observed differences in cumulative weight gains between thermoneutral and conventional control groups, but body weights poorly segregated among genotypes in thermoneutral mice, whereas differences had clearly established in mice raised conventionally *(Figure 6C)*. Furthermore, even if a small difference in body weight still persisted between thermoneutral *Adpn⁺/LAL⁻* and *Adpn⁺/LAL⁺* groups, this was not related to lower fat mass, but decreased in lean mass preexisting before thermoneutrality was applied *(Figure 6D)*. Lowering of cholesterolemia in conventionally raised LAL overexpressing mice *(Figure 5E)* was no longer present after thermoneutral housing (*Figure 6~~D~~E)*, nor amelioration of glucose tolerance *(Figure 6~~E~~F)*. Thus, LAL mice phenotype is highly dependent on housing temperature, which demonstrated a role for adipocyte thermogenic activity and led us to focus on brown/beige adipose tissue depots as preferential functional targets of LAL overexpression.

*LAL overexpression modulates adipocyte cholesterol homeostasis and induces mitochondrial steroidogenesis.*

Investigating BAT closer, we found no significant change in TG contents between *Adpn⁺/LAL⁺* and control mice *(Figure 7A)*, but free cholesterol was increased ~~had accumulated~~ in the BAT of LAL overexpressing mice *(Figure 7B)*. Free cholesterol represents the major fraction of total cholesterol in BAT (81.7+/-6.1% and 83.0+/-3.7% in *Adpn⁺/LAL⁺* and controls respectively), far above the esterified cholesterol form *(Figure 7B insert)*. Selective impact on BAT was suggested, as no change with LAL overexpression was found in the white OvAT *(Supplemental figure ~~4~~3)*. In BAT of *Adpn⁺/LAL⁺* mice, cholesterol-regulated *Ldlr* and *Hmgcr* mRNA expression genes were down-regulated compared to controls, and *Srebf2* expression followed the same trend, although not reaching the statistical significance threshold *(Figure 7C)*. Genes controlling cholesterol efflux (*Abca1* and *Scarb1*) were not induced *(Figure 7D)*~~.~~ ~~Together, attenuation of SREBP tone in LAL overexpressing mice (a situation mirroring activated SREBP in *Lipa* knocked-down cultured adipocytes, as seen above), and unaffected cholesterol efflux is~~ consistent with tissue free cholesterol accumulation. We also observed that compared to control BAT, LAL overexpressing BAT expressed lower levels of ER stress markers, suggesting ameliorated metabolic adaptation *(Figure 7E)*. In agreement, BAT *Ucp1*mRNA expression positively associated with LAL expression *(Figure 7F)*. Regarding ScAT, a white fat depot in which brown-like adipocytes can develop (a process called fat beig~~e~~ing) we could also detect positive *Ucp1* mRNA expression in 40% of the *Adpn⁺/LAL⁺* mice, compared to less

than 10% in controls *(Figure 7G)*. Also, a trend toward higher proportion of fat tissue positive for *Cidea* and *Dio2* mRNA was found in SCAT of *Adpn*$^{+}$*/LAL*$^{+}$ (*Figure 7G*), suggesting a higher potential for beiging. Together these data indicate that LAL overexpression improved thermogenic potential ~~BAT activity~~.

BAT activation fits with a leaner phenotype of LAL overexpressing mice on HFD, but surprisingly coexists with tissue free cholesterol accumulation, which is usually considered ~~reported~~ a deleterious condition for mitochondrial function (19). Nonetheless, the inner mitochondrial membrane is equipped with a steroidogenic enzyme machinery, which transforms free cholesterol into steroids, a pathway that has the potential to alleviate mitochondrial cholesterol overload. The gene encoding the first step in steroidogenesis, the mitochondrial P450 side-chain cleavage enzyme *Cyp11a1*, which converts cholesterol into pregnenolone is expressed in brown adipocytes (20). We found that the expression of this~~two~~ steroidogenic genes: *Cyp11a1* as well as its upstream transcriptional regulator *Nr5a1 (*known as steroidogenic factor 1) were upregulated in BAT of LAL overexpressing mice *(Figure 7H)*. In addition, BAT *Nr5a1* expression positively associated with LAL *(Figure 7I)*, and was negatively linked to body weight gain on HFD *(Figure 7J)*. Mass spectrometry profiling of serum steroids indicated a trend towards higher pregnenolone and 17-OH pregnenolone concentrations in LAL overexpessing mice compared to controls *(Figure 8A-B)*. Further, 5α-dihydrotestosterone (5ADT) and testosterone, downstream products of pregnenolone in the sex hormone branch of steroidogenesis were significantly higher in *Adpn*$^{+}$*/LAL*$^{+}$ mice serum *(Figure 8C-D). 17OH-pregnenolone* and 5ADT positively correlated with BAT *Nr5a1* mRNA expression *(Figure 8E-F)*. Other serum metabolites in the corticosteroid or mineralosteroid pathways remained unchanged in the two groups of mice (not shown). Altogether, these data reveal induction of BAT mitochondrial steroidogenesis, likely an adaptive response to accelerated cholesterol utilization in BAT following LAL overexpression. This potentially explains why mitochondrial function is preserved in cholesterol laden BAT of LAL overexpressing mice. It also provides a molecular basis for the role of BAT as a cholesterol sink, which remain to be further characterized.

**Discussion**

Our study brings novel insights into the unappreciated role of adipocyte lysosomal lipase in energy balance regulation. Previous report in mice with LAL global loss of function demonstrated lipotoxic fattening of organs, especially liver and intestine (21). As models for life threatening Wolman disease in patients, these mice could be normalized by hepatocyte LAL rescue (22). Also, liver-specific gene deletion of LAL revealed that cholesterol esters were the most prominent lipids accumulated in hepatocytes, far above triglycerides and retinyl esters, other *in vitro* LAL substrates (23). Global LAL deficiency was reported to cause disappearance of adipose tissue stores (21), which led to the conclusion that LAL positively regulated adipose tissue storage. However, lipoatrophy in global LAL deficiency is paradoxical, largely due to malabsorptive cachexia and liver failure at the end point of disease development. More recently, it was shown that fat mass was still preserved in young LAL-deficient mice, but reported hypothermic events and defective brown adipose tissue thermogenesis (24), which is in line with our present observations.

Our data reveal a metabolic role of adipose LAL modulation. We demonstrate that LAL regulates energy expenditure and subsequent adipose tissue triglyceride storage, primarily as a gatekeeper of lysosome cholesterol exit for delivery into adipocytes. When adipocyte LAL expression decreases, cholesterol delivery from lysosomes to ER is reduced, which in turn activates cholesterol-dependent SREBP ~~tone~~ and subsequent fat storage. On the contrary,

LAL overexpression, by increasing the turnover of cholesterol through the lysosomal-ER axis, promotes beneficial brown fat activity and a mitochondrial steroidogenic pathway. LAL knock-down in adipose cell lines and overexpression in mice led to apparently different end points (increased fat storage or activated BAT thermogenesis) which can appear unrelated one from the other. However a common pattern in these two opposite situations is the modulation of cholesterol-dependent SREBP pathway *(Figure 8G).* A limitation of our study is lack of information on LAL protein levels or enzyme activity. We could not validate consistent LAL immunoreactivity in adipose tissue extracts despite attempts with several commercial antibodies. Accurate measurement of enzyme activity was also confounded by the unusual status of adipose tissue lipase equipment, which contains, in addition to LAL, a large variety of other very abundant lipases that can still exhibit residual activity at acidic pH. In such a context of tissue equipment with diverse lipases, the accuracy of Lalistat, the “specific” LAL inhibitor is not validated, and the artificial LAL substrate designed in the LAL assay is competed by uncontrolled adipose TG, which further confounds enzyme activity determination.

Our data highlight LAL-dependent regulation of adipocyte cholesterol balance, in line with previous studies on the importance of ABCA1 (25) and ABCG1-mediated cholesterol efflux (26) in fat cell lipid storage. LAL-dependent cholesterol regulation is closely linked to a unique adipocyte low capacity for endogenous cholesterol synthesis (27)(28), leading to inability to restore homeostasis with *de novo* synthetized cholesterol. The LAL-dependent pathway for exogenous cholesterol delivery to adipocytes is responsive to nutritional overload in obesity. We show here that in mice on HFD, BAT cholesterol content is LAL-dependent, as well as body weight gain. Although direct subcellular localization of cholesterol accumulation upon LAL manipulations would have reinforced our conclusions, indirect biochemical quantifications confirm that free cholesterol is indeed accumulated in LAL overexpressing fat cells. Together with BAT cholesterol accumulation in LAL overexpressing mice, we found lower cholesterolemia which might suggest that activated BAT serves as a metabolic sink for cholesterol, as it does for glucose, fatty acids (29) and branched chain amino acids (30). Indeed, protective brown fat activation against hypercholesterolemia has been proposed (31). LAL is required for lipophagy, but we found autophagy-independent LAL-dependent regulation in adipocytes. This fits with a minor role of adipocyte autophagic degradation of lipid droplets in face of the prominent importance of cytoplasmic lipases for adipocyte TG mobilization, even if autophagic clearance of other cell components is central for adipocyte maintenance and response to obesity (32) (33)(13).

By exploring LAL status of human adipocytes, we show that as far as the confounding contribution of adipose tissue macrophage LAL is eliminated, LAL expression is reduced in obese adipocytes, which opens the perspective of therapeutic LAL activation. With brown fat as a preferred adipose target, LAL activation could ameliorate metabolic condition in obese subjects if combined with interventions aimed at favoring brown/beige fat stimulation. Further, beneficial lowering of blood cholesterol levels could be expected from the mouse study. Association between cholesterolemia and adipocyte LAL in the obese population explored here could not be investigated because most patients were under statin treatment. Altogether, our present observations argue for considering LAL activation in the obese setting as a strategy to implement protective effects of brown fat activation against metabolic disorders.

**Acknowledgments**. Adpn-rtTa mice were provided by P. Scherer. We thank the members of the Mouse Genetics Engineering of the Institut Pasteur for technical support with transgenic mice. Marie Lhomme (ICAN Analytics Lipidomic facility,La Pitié-Salpetrière,

Paris) is acknowledged for providing fatty acid analysis.
Author contribution: CG, CR, AL, FLV performed the experiments. KC, ELM, LYC an ID designed the experiments and wrote the manuscript. ID is the guarantor of the study.
The funding of National Research Agency (ANR-14-CE12-0017, LIPOCAMD) is acknowledged. No conflict of interest is declared.

**Reference List**

1. Burton BK, Deegan PB, Enns GM, Guardamagna O, Horslen S, Hovingh GK, et al. Clinical Features of Lysosomal Acid Lipase Deficiency. J Pediatr Gastroenterol Nutr. 2015;61(6):619–25.
2. Viaud M, Ivanov S, Vujic N, Duta-Mare M, Aira L-E, Barouillet T, et al. Lysosomal Cholesterol Hydrolysis Couples Efferocytosis to Anti-Inflammatory Oxysterol Production. Circ Res. 2018;122(10):1369–84.
3. Huang SCC, Everts B, Ivanova Y, O'Sullivan D, Nascimento M, Smith AM, et al. Cell-intrinsic lysosomal lipolysis is essential for alternative activation of macrophages. Nat Immunol. 2014;15(9):846–55.
4. Coronary Artery Disease (C4D) Genetics Consortium. A genome-wide association study in Europeans and South Asians identifies five new loci for coronary artery disease. Nat Genet. 2011;43(4):339–44.
5. Zechner R, Madeo F. Cell biology: Another way to get rid of fat. Vol. 458, Nature. 2009. p. 1118–9.
6. Singh R, Kaushik S, Wang Y, Xiang Y, Novak I, Komatsu M, et al. Autophagy regulates lipid metabolism. Nature. 2009;458(7242):1131–5.
7. Coupé B, Ishii Y, Dietrich MO, Komatsu M, Horvath TL, Bouret SG. Loss of autophagy in pro-opiomelanocortin neurons perturbs axon growth and causes metabolic dysregulation. Cell Metab. 2012;15(2):247–55.
8. Ouimet M, Franklin V, Mak E, Liao X, Tabas I, Marcel YL. Autophagy regulates cholesterol efflux from macrophage foam cells via lysosomal acid lipase. Cell Metab. 2011;13(6):655–67.
9. Schweiger M, Schreiber R, Haemmerle G, Lass A, Fledelius C, Jacobsen P, et al. Adipose triglyceride lipase and hormone-sensitive lipase are the major enzymes in adipose tissue triacylglycerol catabolism. J Biol Chem. 2006;281(52):40236–41.
10. Zimmermann R, Strauss JG, Haemmerle G, Schoiswohl G, Birner-Gruenberger R, Riederer M, et al. Fat mobilization in adipose tissue is promoted by adipose triglyceride lipase. Science (80- ). 2004;306(5700):1383–6.
11. Marcelin G, Da Cunha C, Gamblin C, Suffee N, Rouault C, Leclerc A, et al. Autophagy inhibition blunts PDGFRA adipose progenitors' cell-autonomous fibrogenic response to high-fat diet. Autophagy. 2020;
12. Fiet J, Bouc Y Le, Guéchot J, Hélin N, Maubert MA, Farabos D, et al. A liquid chromatography/tandem mass spectometry profile of 16 serum steroids, Including 21-Deoxycortisol and 21-deoxycorticosterone, for management of congenital adrenal hyperplasia. J Endocr Soc. 2017;1(3):186–201.
13. Soussi H, Reggio S, Alili R, Prado C, Mutel S, Pini M, et al. DAPK2 downregulation associates with attenuated adipocyte autophagic clearance in human obesity. Diabetes. 2015;64(10):3452–63.
14. Xu X, Grijalva A, Skowronski A, Van Eijk M, Serlie MJ, Ferrante AW. Obesity activates a program of lysosomal-dependent lipid metabolism in adipose tissue macrophages independently of classic activation. Cell Metab. 2013;18(6):816–30.
15. Marcelin G, Ferreira A, Liu Y, Atlan M, Aron-Wisnewsky J, Pelloux V, et al. A PDGFRα-Mediated Switch toward CD9highAdipocyte Progenitors Controls Obesity-Induced Adipose Tissue Fibrosis. Cell Metab. 2017;25(3):673–85.
16. Schlager S, Vujic N, Korbelius M, Duta-Mare M, Dorow J, Leopold C, et al. Lysosomal lipid hydrolysis provides substrates for lipid mediator synthesis in murine macrophages. Oncotarget. 2017;8(25):40037–51.
17. Heltianu C, Robciuc A, Botez G, Musina C, Stancu C, Sima A V., et al. Modified Low

Density Lipoproteins Decrease the Activity and Expression of Lysosomal Acid Lipase in Human Endothelial and Smooth Muscle Cells. Cell Biochem Biophys. 2011;61(1):209–16.
18. Kaushik S, Cuervo AM. Degradation of lipid droplet-associated proteins by chaperone-mediated autophagy facilitates lipolysis. Nat Cell Biol. 2015;17(6):759–70.
19. Echegoyen S, Oliva EB, Sepulveda J, Diaz-Zagoya JC, Espinosa-Garcia MT, Pardo JP, et al. Cholesterol increase in mitochondria: Its effect on inner-membrane functions, submitochondrial localization and ultrastructural morphology. Biochem J. 1993;289(3):703–8.
20. Li J, Daly E, Campioli E, Wabitsch M, Papadopoulos V. De novo synthesis of steroids and oxysterols in adipocytes. J Biol Chem. 2014;289(2):747–64.
21. Du H, Heur M, Duanmu M, Grabowski GA, Hui DY, Witte DP, et al. Lysosomal acid lipase-deficient mice: depletion of white and brown fat, severe hepatosplenomegaly, and shortened life span. J Lipid Res. 2001;42(4):489–500.
22. Du H, Zhao T, Ding X, Yan C. Hepatocyte-Specific Expression of Human Lysosome Acid Lipase Corrects Liver Inflammation and Tumor Metastasis in lal-/-Mice. Am J Pathol. 2015;185(9):2379–89.
23. Pajed L, Wagner C, Taschler U, Schreiber R, Kolleritsch S, Fawzy N, et al. Hepatocyte-specific deletion of lysosomal acid lipase leads to cholesteryl ester but not triglyceride or retinyl ester accumulation. J Biol Chem. 2019;294(23):9118–33.
24. Duta-Mare M, Sachdev V, Leopold C, Kolb D, Vujic N, Korbelius M, et al. Lysosomal acid lipase regulates fatty acid channeling in brown adipose tissue to maintain thermogenesis. Biochim Biophys Acta - Mol Cell Biol Lipids. 2018;1863(4):467–78.
25. Le Lay S, Robichon C, Le Liepvre X, Dagher G, Ferre P, Dugail I. Regulation of ABCA1 expression and cholesterol efflux during adipose differentiation of 3T3-L1 cells. J Lipid Res. 2003;44(8).
26. Frisdal E, Le Lay S, Hooton H, Poupel L, Olivier M, Alili R, et al. Adipocyte ATP-binding cassette G1 promotes triglyceride storage, fat mass growth, and human obesity. Diabetes. 2015;64(3).
27. Le Lay S, Ferré P, Dugail I. Adipocyte cholesterol balance in obesity. Biochem Soc Trans. 2004;32(1):103–6.
28. Dugail I, Le Lay S, Varret M, Le Liepvre X, Dagher G, Ferré P. New insights into how adipocytes sense their triglyceride stores. Is cholesterol a signal? Horm Metab Res. 2003;35(4):204–10.
29. Cypess AM, Lehman S, Williams G, Tal I, Rodman D, Goldfine AB, et al. Identification and importance of brown adipose tissue in adult humans. N Engl J Med. 2009;360(15):1509–17.
30. Yoneshiro T, Wang Q, Tajima K, Matsushita M, Maki H, Igarashi K, et al. BCAA catabolism in brown fat controls energy homeostasis through SLC25A44. Nature. 2019;572(7771):614–9.
31. Berbeé JFP, Boon MR, Khedoe PPSJ, Bartelt A, Schlein C, Worthmann A, et al. Brown fat activation reduces hypercholesterolaemia and protects from atherosclerosis development. Nat Commun. 2015;10(6):6356.
32. Le Lay S, Briand N, Blouin CM, Chateau D, Prado C, Lasnier F, et al. The lipoatrophic caveolin-1 deficient mouse model reveals autophagy in mature adipocytes. Autophagy. 2010;6(6):754–63.
33. Soussi H, Clément K, Dugail I. Adipose tissue autophagy status in obesity: Expression and flux—two faces of the picture. Autophagy. 2016;12(3):588–9.

## Figure Legends

**Figure 1:** *Adipocyte LAL expression is decreaseds in obesity.*
(**A**) Adipose tissue *Lipa* mRNA expression in diet-induced murine obesity. Mice were fed control chow (n=5) or a high fat diet (n=8) for 12 weeks before mRNA extraction from subcutaneous adipose tissue. floating adipocytes or SVF cells after collagenase digestion of epididymal mice adipose tissue and (**B**) Lipa mRNA in floating adipocytes or in cell subsets after SVF cells fractionation by FACS. Four independent experiments on pooled epididymal adipose tissue digested with collagenase are shown. (**C**) *LIPA* mRNA expression in human subcutaneous adipose tissue SVF cells after collagenase digestion. Each point represents a preparation from a single donor, plotted against the BMI of the subject. The characteristics of the obese group is described in Table 1 (see group1). SVF from nine non-obese subjects (age 31.2 +/-3.3 years, mean BMI 21.7 +/- 0.6 Kg/m$^2$) was also analyzed. No difference between lean (black dots) or obese (open dots) donors were found. (**D**) *LIPA* mRNA expression in floating adipocytes of lean or obese subjects. Only lipoaspirated subcutaneous fat tissue was available from lean subjects undergoing lipoaspiration, whereas subcutaneous and visceral (omental) fat were collected in obese patients undergoing bariatric surgery. ** indicates statistical ($p<0.01$) difference by Mann Whitney non-parametric test. (**E**) Relationship linking subcutaneous (Sc) and Omental (Om) adipocyte *LIPA* mRNA expression in obese patients. Correlation is highly significant ($r= 0.781$, $p <0.001$). (**F**) Spearman correlations between undigested (unfragmented) adipose tissue LIPA mRNA expression and obesity-related dysfunction markers in a group of 21 massively obese patients described for clinical characteristics, indicated as group 2 in Table 1.

**Figure 2:** *Lentiviral-mediated Lipa inhibition in cultured adipocytes does not affect lysosome function or autophagic flux.*
(**A**) Efficiency of Sh sequences to inhibit *Lipa* expression in differentiated 3T3-L1 adipocytes. Three independent experiments were performed. (**B**) Impact of LAL inhibition on total cholesterol contents (free andor esterified) contents of differentiated adipocytes maintained in standard medium, supplemented or not with 0.1mg/ml OxLDL (ThermoFisher, J65591) for 2 days in standard medium. Mean values +/- sem from three independent experiments are shown, differences between groups were tested by Student's t test. (**C**) Triacylglycerol (TG) content of adipocytes assessed after lipid extraction and , normalizationed to cell proteins. (**D**) Perilipin expression by Western blot analysis. The two perilipin isoforms were quantified and normalized totο ßb-actin signals. Bars represent mean values +/- sem of three independent determinations. * indicate significant differences by Student's t test. (**E**) Lysosome imaging of living adipocytes after pulse labelling for 4 hour with 0.3mg/ml 10,000MW Dextran Texas–Red (Molecular Probes, D1863) followed by 2-hours chase and fixation. Immunolabelling with Perilipin immunolabelling was followed by incubation with 300nM DAPI (ThermoFicher, D3571) was included before mounting in Fluoromount-G (Sothern-Biotech, 0100-01). Red fluorescence intensity was quantified in delineated cells and normalized to surface area using image J. (**F)** Western blot analysis of LC3-II and p62 protein contents in cells exposed or not to lysosome inhibitors to assess autophagic flux. Each lane represents independently generated stably transfected population. Bafilomycin A1 (BAF, 0.1µM) or Chloroquine (CLQ, 25µM) were added for 4 hours. (**G-H**) Quantification of western blots signals after b-actin normalization to ß-actin. Values are mean +/- sem from at least three independent cell pools, each normalized to control condition with no lysosome inhibitor. **(I-K)** Lipolytic rates were determined under basal (I) or isoproterenol-stimulated

conditions, in the presence or absence of Bafilomycin (BAF) to inhibit lysosomes (J-K). Experiments were repeated 3-4 times. Values are mean +/- sem.

**Figure 3:** *Stable LAL knock-down affects adipocyte cholesterol homeostasis.*
(**A**) Stratification of stable transfectants according to *Lipa* residual expression. A total of 17 independent cell pools were analyzed for *Lipa* mRNA and assigned one of the three groups by comparison with parental non transfected controls. (**B**) RT-qPCR determination of cholesterol-regulated genes mRNA in cell groups with gradual *Lipa* inhibition. Significant differences by Student t test are shown. (**C**) Spearman correlation of *Srebf2* mRNA and *Lipa* residual expression. Correlation coefficient is indicated~~shown~~, p<0.05. (**D**) Pretreatment of cells with exogenous free cholesterol to replenish intracellular pools was performed by adding 1mg/ml cholesterol (Sigma-Aldrich, C3045) in DMEM containing 1% of fatty acid free bovine serum albumin for 1-hour. Medium was removed and cells were incubated in fresh medium for subsequent 4-hours before lysis. *Hmgcr* and *Srebf2* mRNA were assessed as above. (**E**) Perilipin fluorescence intensity normalized to cell area was quantified ~~Lipid droplet imaging by perilipin fluorescence~~ in *Lipa* deficient cells and controls. (**F**) FAS protein content was assessed by western blot in clones with different degrees of Lipa inhibition, and normalized to ßactin.~~Perilipin fluorescence intensity normalized to cell area was quantified.~~
(**G**) Lipid droplet diameter measurement using PerfectImage Software (Claravision). Each point represents mean diameter values+/- sem of independent cell pools, plotted against *Lipa* residual expression. Statistically significant (p<0.05) negative correlation linking LAL expression and LD size is shown with correlation coefficient. ER stress markers *Grp78* (**H**) and *Atf4* (**I**) mRNA were assessed ~~as ER stress marker~~ following cell incubation for 6h in serum-free medium before addition of 0.5mM Dithiothréitol (Invitrogen, D1532) for 1hour. Three independent experiments were performed, with 6 independent stable transformants in each group. V~~v~~alues are means+/- sem, normalized to 18S RNA. ~~ER stress was induced by.~~

**Figure 4:** *Validation of adipose-specific LAL overexpression in mice.*
(**A-B**)~~:~~ RT-qPCR expression of total LAL (endogenous plus transgenic) mRNA in adipose depots and liver of female (**A)** and male (**B**) mice. Three adipose depots: gonadal fat (Ovarian (OvAT) or Epididymal (EpiAT)), Subcutaneous (ScAT) and Brown (BAT) adipose tissues were evaluated in female and male mice of indicated genotypes. Statistical differences between genotypes by Student's t test are shown. (**C**) Linear regression plots indicating strong dependence of total LAL expression to transgenic LAL mRNA in adipose tissues of female mice. Correlation coefficients and p values are indicated for each tissue. (**D**) Body composition ~~Body weight gain~~ (**E**) Body weight gain ~~body composition~~ and (**F**) adiposity of female mice fed a HFD for 12 weeks. **(G)** ScAT lipolysis was assessed *ex vivo* by measuring glycerol release from tissue fragments in the presence or not of $10^{-5}$M isoproterenol. Incubation was for 2 hours at 37°C in humidified atmosphere with 5% $CO_2$. Lipolytic activity was normalized to tissue weight.

**Figure 5:** *Metabolic phenotype of adipose-specific LAL overexpressing mice.*
(**A**) mRNA expression of inflammation markers in ovarian adipose tissue by RT-qPCR. (**B**) Fasting glycemia and (**C**) oral glucose tolerance (glucose load 2g/kg) were assessed after food withdrawal for 6 hours. * indicate differences between groups by Student's t test. (**D**) Correlation linking fasting glycemia and serum cholesterol in HFD fed mice. (**E**)

Cholesterolemia and (**F**) Triglyceridemia were assessed as described in methods. **(G-H)** Indirect calorimetry was performed in HFD fed mice, maintained at room temperature. Five mice in each group were followed during five consecutive days. (**G**) Mean 24-h food intake and locomotor activity during day or night time were recorded. (**H**) Energy expenditure was calculated from gas respiratory exchange data. (**I**) Relationship linking body weight gain during HFD and total LAL expression in BAT.

**Figure 6:** *LAL mice phenotype at thermoneutrality.*
(**A**) Preservation of genotype-dependent LAL expression in mice kept at thermoneutrality for 4 weeks. (**B**) BAT morphology in~~from~~ HFD mice housed at room temperature or thermoneutrality (white area are lipid droplets). **(C)** Inter-genotype comparisons of body weight changes in mice raised conventionally or housed at thermoneutrality (30°). **(D)** Body composition of mice maintained at thermoneutrality for 4 weeks on HFD. Of note, inter-genotype differences in body weight are linked to preexisting differences in lean mass but not fat. **(E)** Cholesterolemia and **(F~~E~~)** glucose tolerance assessed by OGGT on HFD mice maintained at thermoneutrality for 4 weeks.

**Figure 7:** *LAL overexpression regulates BAT cholesterol homeostasis.*
After lipid extraction, BAT triglyceride (**A**), and~~or~~ BAT free cholesterol **(B)** were~~as~~ assessed in conventional mice fed HFD ~~kept at room temperature~~. inset shows unchanged min to max of esterified cholesterol values (as the difference from total to free cholesterol determinations). Significant differences by Student's t test are indicated. (**C**) BAT mRNA expression of SREBP-regulated genes ~~(**C**)~~, (**D**) genes related to cholesterol efflux, ~~(**D**)~~ and UPR markers ~~genes~~ (**E**) ~~are shown~~. Statistical differences by Student's t test are indicated. (**F**) Spearman correlation linking *Ucp1* mRNA and LAL expression in BAT samples. (**G**) ~~ScAT~~ *Ucp1, Cidea and Dio2* mRNA were~~as~~ assessed in ~~a total of 36~~ ScAT of female mice raised at room temperature~~,~~ (14-16 per group) and plotted as violin plots to visualize heterogeneity of individual values between groups.~~and percentage of Ucp1 positive tissues was plotted for each genotype, indicating increased frequency in Adpn+/LAL+ mice.~~ (**H**) BAT expression of steroidogenic genes by RT-qPCR. Significant differences by Student's t test are indicated. (**I**) Spearman correlation~~s~~ of *Nr5a1* mRNA expression to BAT LAL expression ~~in BAT~~ or ~~(**J**)~~ b~~B~~ody weight gain on HFD (**J**).

**Figure 8:** *Cholesterol-derived serum steroids in LAL overexpressing mice.*
Pregnenolone **(A)** 17-OHpregnenolone **(B)**, 5α-dihydrotestosterone **(C)**, and Testosterone **(D)** concentrations in mice serum were expressed as ng/ml. * indicates significant difference between groups ($p<0.05$) by Student's t test. Spearman correlations between BAT *Nr5a1* mRNA expression and serum 17-OHpregnenolone **(E)** or 5α-dihydrotestosterone **(F)**. **(G)** SREBP target genes response reflecting intracellular cholesterol gauge as a common mechanism underlying the impact of adipose LAL overexpression or knock-down in the models used in this study. In LAL overexpression, accelerated cholesterol uptake is suggested by low blood cholesterol levels. In the human situation, non-obese and obese subjects exhibit differences in adipocyte LAL expression, suggesting potential benefice in therapeutical LAL activation.

**Table 1**: **Clinical characteristics of obese patients**

| | Group 1 (n=45) | | Group 2 (n=21) | |
|---|---|---|---|---|
| | **mean** | **sem** | **mean** | **sem** |
| Age (Years) | 45.4 | 2.16 | 45.7 | 3.04 |
| BMI Kg/M2 | 47.22 | 1.30 | 46.88 | 1.90 |
| Fat Mass % | 49.64 | 0.57 | 48.96 | 0.88 |
| Fasting glucose (mM) | 6.11 | 0.28 | 5.72 | 0.28 |
| Fasting Insullin (µUI/ml) | 21.44 | 2.17 | 25.13 | 3.25 |
| HbA1c (%) | 6.47 | 0.21 | 6.105 | 0.21 |
| Cholesterolemia (mM) | 4.11 | 0.24 | 4.63 | 0.24 |
| Triglyceridemia (mM) | 1.64 | 0.14 | 1.71 | 0.22 |
| HDL Cholesterol (mM) | 1.15 | 0.05 | 1.04 | 0.07 |
| ASAT (IU/l) | 30.94 | 2.95 | 29.47 | 4.76 |
| ALAT (IU/l) | 35.67 | 7.30 | 41.11 | 14.59 |
| GGT (mg/dl) | 46.1 | 7.34 | 46.40 | 12.00 |
| Leptinemia (ng/ml) | 73.8 | 6.50 | 85.16 | 11.39 |
| Adiponectinemia (µg/ml) | 4.07 | 0.30 | 4.23 | 0.32 |
| IL6 (pg/ml) | 5.08 | 0.53 | 4.48 | 0.48 |

Group 1: AT samples were directly frozen and used for LIPA mRNA expression in unfractionated adipose tissue.
Group 2: Freshly collected AT samples were digested with collagenase to separate isolated adipocytes and stroma vascular cell fractions for further investigation of the topology of LIPA expression in cell subfracti0ns.